Physiological characteristics and transcriptomic analysis of response patterns of Gynura divaricata under NaCl stress

Yujie Zeng
South China Institute of Botany

Yuping Xiong
South China Institute of Botany

Junyu Liu
South China Institute of Botany

Xiaohong Chen
South China Institute of Botany

Jianrong Li
South China Institute of Botany

Shuguang Jian
South China Institute of Botany

Hai Ren
South China Institute of Botany

Xinhua Zhang
South China Institute of Botany

Yuan Li
South China Institute of Botany

Zhan Bian
South China Institute of Botany

Kunlin Wu
South China Institute of Botany

Songjun Zeng
South China Institute of Botany

Jaime A. Teixeira Silva
Kagawa University

Guohua Ma

magh@scib.ac.cn

Chinese Academy of Sciences

Research Article

Additional Declarations: No competing interests reported.

Abstract

Soil salinity is a major environmental stress that restricts agricultural production worldwide. *Gynura divaricata* is widely cultivated on tropical islands in China and has both edible and medicinal value. NaCl stress and growth indicators, antioxidant enzyme activity, as well as MDA, proline, and soluble sugar content, were determined. Based on the transcriptomic data of *G. divaricata* tissue-cultured plantlets grown in control (0 mM NaCl) and (50 and 200 mM) NaCl stress conditions, the expression patterns of responsive genes were explored. KEGG enrichment analysis of differentially expressed genes indicated that plant hormone signaling, the MAPK signaling pathway, and starch and sucrose metabolism pathways, were significantly enriched, allowing the main biological pathways and salt stress-responsive genes of *G. divaricata* to be identified, and providing a molecular basis for breeding salt-tolerant varieties.

Introduction

Soil salinity is a major abiotic stress that limits crop productivity globally such that by 2050, it is predicted that nearly half of the world's arable land will be salinized (Butcher et al. 2016). In a high-salt environment, plants are subjected to oxidative and ion stresses due to an increase in reactive oxygen species, Na^+ and Cl^-, causing physiological and biochemical metabolic disorders and resulting in the accumulation of toxic substances, ultimately negatively affecting cell growth and metabolism (Derakhshani et al. 2020; Kulak et al. 2020; Chourasia et al. 2021; Wang et al. 2023). Salinity stress negatively impacts plant growth (Muchate et al. 2016) by reducing plant biomass, lowering crop yield and quality, and restricting agricultural production (Machado and Serralheiro 2017; Li et al. 2021; Frukh et al. 2020). Therefore, exploring and improving salt tolerance of plants to be one way to fortify the sustainable development of food around the world.

Gynura divaricata (L.) DC. (Asteraceae) is distributed in southern and southwest China, and Taiwan (Flora of China Editorial Committee 1999). It does not have strict temperature or soil requirements, and displays strong reproductive ability and stress resistance (Yang and Liu 1998). The roots, stems, leaves and other parts of *G. divaricata* are used medicinally (Li et al. 2009; Wan et al. 2011; Chou et al. 2012; Chen et al. 2014), while the stems and leaves are edible (Yang and Liu 1998). In soil with a low salt content, *G. divaricata* is still able to produce a high content of total sugars, flavonoids, vitamins and other nutrients, serving a dual purpose of food and nutrition as well as soil restoration, leading to its use as a restoration plant in salt-affected arid and barren areas (Wang 2017).

There is only one report on the salt tolerance of *G. divaricata* that examined its morphological and physiological responses to seawater stress (Wang et al. 2017). In that study, as the volumetric concentration of seawater with a mean salt concentration of 3.5% was ≤ 30%, the morphology and physiological activities of *G. divaricata* were normal, but when concentration was ≥ 40%, growth was significantly inhibited, photosynthesis and solute transport were inhibited, membrane functionality was disrupted, antioxidant activity decreased, and malondialdehyde (MDA) accumulated. No study on the molecular biology of salt tolerance in *G. divaricata* has yet been reported.

At present, most research on salt tolerance of island plants has focused on their tolerance to salt stress, morphological adaptations, and physiological changes. Under a range of salt stress, the biomass and photosynthetic parameters of island plants were negatively correlated, and sodium ions accumulated (Feng et al. 2021). Under salt stress, plant growth and development are inhibited due to ionic toxicity caused by osmotic stress. Salinity stress leads to physiological changes in plants, including nutritional imbalance, reactive oxygen species (ROS)-induced damage, damage to membranes, and decreased photosynthetic activity (Chourasia et al. 2021). Excess ROS can lead to increased plasma membrane permeability and extravasation of substances, resulting in water imbalance and separation of the plasma-wall, but plants can cope with salinity-mediated oxidative stress by enhancing enzymatic and non-enzymatic antioxidant activity, which increases antioxidant enzyme activity, as well as proline and MDA content (Chourasia et al. 2021). During the *ex vivo* culture of six halophytes under NaCl stress, antioxidant enzyme activity and proline content increased (Xiong et al. 2019a).

A plant's tolerance to salt does not depend on a single gene, but is influenced by multiple genes. Transcriptome sequencing is widely used to analyze plants' responses to salt stress because it can reflect the molecular response and regulatory network of plants under salt stress at a holistic level. A transcriptomic analysis of *Cynodon dactylon* grown under salt stress showed that several transcription factor (TF) families (MYB, bHLH, WRKY) were expressed differently in root tips, and candidate genes were involved in regulating lignin synthesis, peroxidase-mediated ROS balance, and promoting cell wall loosening (Hu et al. 2015a). Genes associated with ion transport, the removal of ROS, energy metabolism, hormone responses, and other functions purportedly played an important role in the adaptation of *Halogeton glomeratus* to salt stress (Wang et al. 2015). Differentially expressed genes (DEGs) in response to salt stress were significantly enriched in single organism processes, membranes, catalytic activity, and plant hormone signaling pathways in *Clerodendrum inerme* following exposure to salt stress (Xiong et al. 2019). *C. inerme* adapted to early stages of salt stress by regulating the metabolism of nucleotides, amino acids, carbohydrates, enzymes, TFs and plant hormones (Liang et al. 2022). In *Zoysia japonica*, the key genes involved in salt stress response in leaves and roots mainly belong to hormonal pathways, various TF families and DUF families (Wang et al. 2020a).

The objective of this study was to investigate some physiological characteristics such as antioxidant enzyme activity, as well as MDA, proline, and soluble sugar content and gain a transcriptomic appreciation of the molecular network of DEGs involved in the response of *G. divaricata* to salt (NaCl) stress.

Materials and Methods

Plant material: origin and culture

G. divaricata seedlings originated from the Xisha Islands in Hainan, China. After propagation and growing at the Wenchang propagation base in Hainan for six months, they were introduced to the scientific research greenhouse of the South China Botanical Garden, Chinese Academy of Sciences, in Guangzhou, for cultivation management. Stem explants (1.0 cm long) were sterilized with 75% ethanol for 30 sec, washed three times in sterilized distilled water, immersed in

0.1% $HgCl_2$ solution for 15 min, and rinsed with sterilized distilled water five times. Stem segments (including nodes and internodes), which served as explants, were inoculated vertically onto Murashige and Skoog (MS) medium (Murashige and Skoog 1962) (Chembase, Beijing, China) containing 0.5 mg L^{-1} 6-benzyladenine (BA) (Sigma-Aldrich®, St. Louis, MO, USA). Culture jars (350 mL) held 50 mL of basal medium, which contained 30 g L^{-1} sucrose (Sinopharm, Beijing, China) and 3 g L^{-1} carrageenan (Qingdao Jiaquan, Shandong, China). Medium pH was adjusted to 6.0 before autoclaving. Six explants were cultured in each culture jar. The culture room's controlled conditions were: 25 ± 1°C; 12-h photoperiod; light intensity of 80 µmol m^{-2} s^{-1} PPFD. New axillary shoot buds, which formed within 30−50 d, were subcultured on MS medium with 0.5 mg L^{-1} BA to multiply and proliferate shoots for subsequent experiments.

NaCl stress and growth indicators

Rooting medium was MS supplemented with 0.5 mg L^{-1} indole-3-butyric acid (IBA) and different concentrations of NaCl (0, 50, 100, 200, 300, 400 mM) (Analytically pure, Chembase). Shoots (six per culture jar) about 1 cm long and with 4−5 leaves were inoculated into rooting media, with six shoots per culture jar and five culture jars per treatment. After incubation for 3 wk, rooted plantlets were rinsed and wiped dry, and growth indicators (means from 30 shoots) (rooting percentage, mortality percentage, root number, root length, plant height, above-ground fresh weight (biomass), and water content) were investigated for each treatment. The water content was calculated as: [fresh plantlet weigh − dried plantlets weight (drying at 80°C to constant weight) / fresh plantlet weight] × 100%.

Antioxidant enzyme activity, and MDA, proline, and soluble sugar content determination

The leaves of *G. divaricata* plants grown in different NaCl concentrations for 3 wks were used for these assays. For each determination, about 0.1 g of fresh leaves (young terminal leaves + older basal leaves) was ground in liquid nitrogen. The powder was used to determine the activity of three antioxidant enzymes, catalase (CAT, EC 1.11.1.6), peroxidase (POD, EC 1.11.1.7), and superoxide dismutase (SOD, EC 1.15.1.1), according to the kits' instructions (Yin et al. 2018; Li et al. 2019; Wang et al. 2019). Kit's instructions were also used to determine proline content (Chen et al. 2019), and soluble sugar content (Zhang et al. 2018), and MDA content (Gu et al. 2018). All kits were purchased from Beijing Solabao Technology Co., Ltd. (Beijing, China).

Na^+, K^+ and Mg^{2+} content determination

G. divaricata leaves were dried at 80°C for 48 h until constant weight. After grinding with liquid nitrogen to a powder, ions were extracted with 1 M HCl for 12 h. After the solution was filtered through qualitative filter paper (Taizhou, Jiangsu, China) and 50 mL was recouped, it was used to determine K^+, Na^+ and Mg^{2+} contents with an flame atomic absorption spectrophotometer (Takahashi et al. 2007).

RNA extraction and cDNA library construction

Total RNA was extracted from 21 d old control and NaCl-treated *G. divaricata* leaves using the Column Plant RNAOUT Extraction kit (TIANDZ, Beijing, China) and treated with DNase I to remove genomic DNA, as suggested by the manufacturer. The concentration and quality of each sample were determined by agarose electrophoresis or an Agilent 2100 bioanalyzer (Agilent Technologies, Palo Alto, CA, USA). The mRNAs were purified from total RNA using magnetic beads with oligo (dT) and fragmented into small pieces (200−300 bp). The cleaved RNA fragments were primed with a random hexamer primer for first- and second-strand cDNA synthesis. After purification, end repair, and ligation to sequencing adapters, 12 cDNA libraries of three biological replicates for each treatment were construct using the Illumina HiSeq 2500 platform by Personal Biotechnology Co., Ltd. (Shanghai, China).

Sequencing and functional annotation

The percentage of unknown nucleotides and base recognition accuracy of more than 99.0% of bases (Q20) was calculated from raw reads. After cleaning the raw reads and discarding low quality reads, Trinity software (version 2.5.1, https://github.com/trinityrnaseq/trinityrnaseq/wiki) was used for the *de novo* assembly of high-quality reads. To annotate sequences obtained by the *de novo* assembly, assembled transcripts were aligned to NCBI non-redundant protein sequences (NR, http://ftp.ncbi.nlm.nih.gov/blast/db/FASTA/), Gene Ontology (GO, (https://www.blast2go.com/), Kyoto Encyclopedia of Genes and Genome (KEGG, KAAS (http://www.genome.jp/tools/kaas/), evolutionary genealogy of genes: Non supervised Orthologous Groups (eggNOG, http://eggnog.embl.de/version_3.0) and swiss prot protein database (Swiss Prot) (http://www.uniprot.org/help/uniprotkb) using BLASTX with a significance threshold of E ≤ 10^{-5}.

Analysis of gene expression levels

Gene expression levels, which were quantified by RNA-seq using Expectation Maximization (RSEM) software (http://deweylab.github.io/RSEM/), were calculated as the number of fragments per kilobase per transcript per million mapped reads method (FPKM). After filtering, the number of transcripts was analyzed by density distribution and a boxplot graph to investigate the expression patterns among all samples. Pearson's correlation between samples was calculated based on FPKM results to determine the operational stability and reliability of the experiment.

Identification and functional annotation of DEGs

DEseq software (http://www.bioconductor.org/packages/release/bioc/html/DESeq.html) was used to determine significant DEGs defined as a fold change (FC) ≥ 2 (*P* < 0.05). Pheatmap software (https://cran.r-project.org/web/packages/pheatmap/index.html) was used to perform hierarchical clustering to determine the expression patterns of DEGs in the libraries. DEGs were mapped to each term of the GO database to detect significantly (*P* < 0.05) enriched GO terms using the hypergeometric test (Eden et al. 2009). The number of DEGs at different NaCl stress levels was also calculated by the hypergeometric test to identify the main pathways involved in NaCl tolerance and to determine significantly (*P* < 0.05) enriched KEGG pathways (Mao et al. 2005).

qRT-PCR analysis

Candidate DEGs, including up-regulated and down-regulated genes in enriched KEGG pathways, were randomly selected for qRT-PCR analysis to validate the transcriptomic data. qRT-PCR was performed on the ABI 7500 Real-time system (ABI, Alameda, CA, USA) using iTaq™ Universal SYBR Green Supermix (Bio-Rad, Foster, CA, USA). Actin was used as the internal control and the $2^{-\Delta\Delta Ct}$ method (Livak and Schmittgen 2001) was employed to analyze differential expression. The qRT-PCR results were obtained from three biological replicates and three technical repeats for each gene and sample.

Statistical analyses

Duncan's multiple range test (DMRT) was used to analyze the data for significant differences following ANOVA. $P \leq 0.05$ was considered significant. Data used indicate the mean ± standard deviation (SD).

Results

Effects of NaCl stress on growth indexes

G. divaricata shoots had a high rooting percentage (98.89%) within 7 d without NaCl, and showed 28.89−83.33% rooting percentage at low NaCl concentrations (50−100 mM). However, at high concentrations (≥ 200 mM), there was basically no rooting within 7 d, when cultured to 21 d, 100% rooting at 0−50 mM NaCl, and no rooting at a high concentration (400 mM NaCl), the abaxial surface of leaves were dark, while leaves themselves were curled and brittle (Fig. 1). Generally, as NaCl concentration increased, rooting percentage decreased (Table 1).

When cultured at 0−300 mM NaCl, there was no plantlet death, but when the NaCl concentration was 400 mM, a small number of plantlets died. The average number of roots and root length decreased as NaCl concentration increased, but average root length increased when the NaCl concentration was 50 mM. Plantlet height decreased from 12.27 cm to 7.89 cm with increasing NaCl concentration. Above-ground biomass per plantlet reached a maximum (245.89 mg) at 200 mM NaCl, and plantlet water content was highest (95.30%) at 50 mM NaCl but gradually decreased to 92.4% at 400 mM NaCl (Table 1).

Antioxidant enzyme activity, and MDA, proline, and soluble sugar content

CAT activity of 50−400 mM NaCl-treated *G. divaricata* leaves was significantly higher than in control leaves, and highest at 50 mM (Fig. 2a). POD activity in the 200-400 mM NaCl treatments was significantly higher than in control leaves, and highest at 400 mM (Fig. 2b). SOD activity in all NaCl treatments was significantly higher than in leaves of the control group, and highest at 300 mM (Fig. 2c). MDA content in all NaCl treatments was significantly higher than in the control group, and highest at 200 mM (Fig. 2d). Except for 50 mM NaCl, proline content in all other NaCl treatments was significantly higher than in the control group, and highest at 200 mM (Fig. 2e). Except for 50 mM, soluble sugar content in all NaCl treatments was significantly lower than in the control group, and lowest at 300 mM (Fig 2f).

Na^+, K^+ and Mg^{2+} content

Na^+ content accumulated significantly in leaves relative to control leaves, reaching a maximum at 200 mM (Fig. 3a). Conversely, K^+ decreased significantly in leaves relative to control leaves, reaching a minimum at 50 and 200 mM (Fig. 3b). Mg^{2+} content decreased significantly at 100, 300 and 400 mM relative to control leaves (Fig. 3c). Na^+ / K^+ content was significantly higher in all NaCl treatments relative to the control, and maximum at 200 mM (Fig. 3d).

Correlation analysis of growth and physiological indicators under NaCl stress

The correlation analysis of growth and physiological indicators of *G. divaricata* leaves in response to different NaCl treatments showed that NaCl concentration was positively correlated with POD activity, as well as Pro, Na^+, and Na^+/K^+ content, but negatively correlated with soluble sugar and Mg^{2+} content, as well as root number, root length, plant height and water content (Table 2).

De novo assembly and sequencing quality analysis

In 0, 50 and 200 mM NaCl stress treatments, 43405450−57982988 clean reads were obtained after filtering the original sequencing data, Q30 exceeded 92.58%, and GC content lay in the 42.91−43.53% range (Table 3). The length distribution of the assembled transcripts and unigenes are shown in Fig. 4.

Total number of annotated unigenes

The total number of unigenes functionally annotated by six databases, NR, GO, KEGG, clusters of orthologous groups (COG), swiss prot protein database (Swiss Prot) and the protein family database (Pfam), was 57297, and 23395 (40.83%), 17564 (30.65%), 11060 (19.30%), 25070 (43.75%), 22,062 (38.50%), and 20982 (36.62%), respectively, with 27588 (48.15%) unigenes annotated to at least one database (Supplementary Table 1).

Among the genes annotated in the NR database, 76.71% (66.45% + 10.26%) had an E value < $1e^{-20}$ (Fig. 5a), and 69.40% (49.48% + 19.92%) had a genetic similarity > 60% (Fig. 5b). 52.32% of the genes were annotated in known species, the most similar species being *Selaginella moellendorffii* (16.53%), followed by *Marchantia polymorpha* (9.64%) (Fig. 5c).

In the GO database, a total of 73360 unigenes were annotated into three categories: molecular functions, biological processes and cellular components, accounting for 29.82%, 34.06% and 36.12%, respectively. In the molecular function category, they were mainly associated with binding and catalytic activity, among biological processes, they were mainly associated with cellular and metabolic processes, and in the cell components category, they were mainly associated with cell and membrane parts, and organelles (Fig. 6a); 73.54% of unigenes were associated with seven categories of GO terms. A total of 7729 unigenes were annotated in in five branches of the KEGG database: metabolism, genetic information processing, environmental information processing,

cellular processes and organism systems, with metabolism accounting for 54.03%; most genes were associated with carbohydrate metabolism, translation, folding, sorting and degradation, amino acid metabolism, and transport and catabolism (Fig. 6b). A total of 13233 unigenes were associated with unknown functions in the COG database while 13399 unigenes were associated with 22 known categories, with the largest number of annotations related to posttranslational modification, protein turnover, chaperones (1790), followed by replication, recombination and repair (1753), signal transduction mechanisms (1648), transcription (1418), and others (Fig. 6c).

Analysis of DEGs

NaCl stress induced the differential expression of genes. As NaCl concentration increased, the number of DEGs in tissue-cultured *G. divaricata* leaves also increased. In the L50 vs CK, L200 vs CK, and L200 vs L50 comparisons, 177 and 128, 1396 and 1158, and 1024 and 940 DEGs were up- and downregulated, respectively (Fig. 7a). The number of unique DEGs in common to all three groups was 80, while 48, 1243 and 772 DEGs were unique to L50 vs CK, L200 vs CK, and L200 vs L50 comparisons, respectively (Fig. 7b).

In the L50 vs CK comparison, mevalonate kinase activity was highest, followed by response to hydrogen peroxide while most DEGs were related to oxidoreductase activity, followed by lipid metabolic processes (Fig. 8a). In the L200 vs CK comparison, highest expression was related to rhythmic processes, followed by photomorphogenesis, while most DEGs were related to DNA binding, followed by transporter activity (Fig. 8b). In the L200 vs L50 comparison, highest expression was related to the ethylene-activated signaling pathway followed by rhythmic processes, while most DEGs were related to DNA binding, followed by transcription regulator activity (Fig. 8c).

KEGG enrichment analysis showed that most DEGs in the L50 vs CK comparison were related to linoleic acid metabolism followed by zeatin biosynthesis (Fig. 9a). In the L200 vs CK and L200 vs L50 comparisons, most DEGs were related to plant hormone signal transduction, MAPK signaling pathway-plant, and starch and sucrose metabolism (Fig. 9b, 9c).

Genetic analysis related to plant hormone signaling, MAPK signaling and starch, sucrose metabolic and ion transport pathways

PYL, PP2Cs and SnRK2s are important components of the abscisic acid pathway. PYL expression was downregulated under salt stress, resulting in the activation of PP2C expression, which inhibited SnRK2s expression. ARF in the auxin pathway and some IAAs and SAURs, CRE1 and A-ARR in the cytokinin pathway, GID1 in the gibberellin pathway and TGA in the salicylic acid (SA) pathway were significantly upregulated (Fig. 10). Seven genes, including TRINITY_DN6033_c0_g1, TRINITY_DN27156_c0_g1 and TRINITY_DN4509_c0_g1 in the MAPK signaling pathway were highly expressed in the 200 mM NaCl treatment while eight genes, including TRINITY_DN2820_c0_g2, TRINITY_DN2815_c0_g2 and TRINITY_DN29407_c0_ g2, were highly expressed only in the control group or in the 50 mM NaCl-treated group (Fig. 11). Under salt stress, the expression of sucrose invertase (INV, sacA), sucrose synthase (SUS), and TRINITY_DN15485_c0_g2 (E2.7.1.4, scrK) was upregulated (Fig. 12).

KEGG enrichment showed that 10 genes associated with the plant hormone signaling pathway, like TRINITY_DN2820_c0_g2, TRINITY_DN2815_c0_g2, and TRINITY_DN29407_c0_g2, were only highly expressed in the control group or in the 50 mM NaCl-treated group, while 15 genes, like TRINITY_DN6033_c0_g1, were highly expressed in the 200 mM NaCl-treated group (Fig. 13a). Nine genes (TRINITY_DN29407_c0_g2, TRINITY_DN2815_c0_g2, TRINITY_DN9614_c0_g1, TRINITY_DN8933_c0_g1, TRINITY_DN4509_c0_g1, TRINITY_DN6033_c0_g1, TRINITY_DN2820_c0_g2, TRINITY_DN14265_c0_g1, TRINITY_DN12556_c0_g1) were co-mediated two pathways, plant hormone signaling and the MAPK pathway (Supplementary Tables 1 and 2). The expression of four PP2Cs in the abscisic acid pathway were up-regulated in response to salt stress, as was one ERF1 in the ethylene pathway, and WRKY22, related to ethylene and hydrogen peroxide responses (Fig. 13b). KEGG enrichment analysis showed that six genes in the starch and sucrose metabolic pathway, including TRINITY_DN4486_c1_g1, TRINITY_DN6333_c0_g1, and TRINITY_DN32855_c1_g2, were highly expressed in the 200 mM NaCl treatment while five genes, including TRINITY_DN209_c0_g1, TRINITY_DN4277_c0_g1, and TRINITY_DN6608_c0_g1, were highly expressed only in the control group (Supplementary Table 3; Fig. 13c). KEGG enrichment analysis showed that eight genes, like TRINITY_DN38284_c0_g1, related to ion transport, were highly expressed in the 200 mM NaCl treatment while five genes, such as TRINITY_DN30952_c0_g2 and TRINITY_DN16375_c0_g1, were highly expressed in the control group (Supplementary Table 4). DEGs included cation transporters (TRK, HKT), sodium-related transporters (chaA, CAX), potassium transporters (kup), magnesium transporters (MRS2, MFM1), and others (Fig. 13d).

Transcription factor analysis

According to the PlantTFDB database, a total of 972 TFs were annotated. These belonged to 33 TF families, mainly MYB (157; 16.15%), AP2/ERF (102; 11.01%), bHLH (78; 8.02%), NAC (70; 7.20%), C2C2 (70; 7.20%) and others (Fig. 14).

Verification of target gene qRT-PCR

To verify the reliability of RNA-seq results, eight DEGs were screened with TRINITY_DN1091_c0_g1 as internal reference gene. TRINITY_DN22392_c0_g1, TRINITY_DN24475_c0_g2, TRINITY_DN43752_c0_g1 and TRINITY_DN4509_c0_g1 were those genes displaying upregulated expression while TRINITY_DN2820_c0_g2, TRINITY_DN8933_c0_g1, TRINITY_DN4277_c0_g1, and TRINITY_DN29407_c0_g2 were genes displaying downregulated expression (Supplementary Table 5). These genes were validated by qRT-PCR analysis. The expression of these eight genes based on qRT-PCR corresponded to their trends in expression as shown by RNA-seq sequencing, indicating that the RNA-seq sequencing results were valid and reliable (Fig. 15).

Discussion

Physiological responses of plants to salt stress

Salt stress tends to negatively impact plant growth, development, and reproduction, and can even induce plant death. Plant phenotype intuitively reflects the positive and negative aspects of a plant's growth environment, and salt stress can cause leaf wilting, darkening, aging, and inhibited growth (Muchate et al. 2016). When a salt mixture (Na_2SO_4, NaCl, $CaCl_2$, $MgSO_4$ in a molar ratio of 9:5:5:1) and EQ levels of 10 and 20 dS m^{-1} increased, the leaf area, stem thickness, plant height and fresh dry weight of several cotton (*Gossypium hirsutum*) cultivars decreased (Qadir and Shams 1997). In order to reduce the loss of water under 25 g L^{-1} NaCl salt stress, the thickness of leaves, the upper epidermis, and palisade tissue of *Guettarda speciosa* increased (Li et al. 2021). *Medicago ruthenica* (L.) Trautv. seedlings partially or completely died in response to the synergistic effect of high salt concentration (24−120 mM NaCl) and high alkali content, and the water content of aboveground organs, the relative growth rate of aboveground organs and roots, and pigment concentration decreased, as did root viability in the high salinity treatment, whereas low salinity promoted root viability (Yang et al. 2011). *G. divaricata* formed roots normally in response to a low concentration (50−100 mM) of NaCl, showing no obvious differences with the control group, and even promoted some growth indicators, which may be due to the ability of low salt concentration to stimulate photosynthesis (Kurban et al. 1999). However, when NaCl concentration exceeded 300 mM, *G. divaricata* could not develop normal roots, the leaves became thick, hard and brittle, and localized tissue death was observed (Fig. 1d).

In plants under salt stress, oxidative stress arises due to an increase in ROS, which plays a dual role, both as a toxic byproduct of aerobic metabolism and as a key regulator of growth, development, and defense pathways (Mittler et al. 2004). As part of the latter function, ROS can be divided into enzymatic and non-enzymatic reaction systems in which the former plays a crucial role in the plant's response to adversity by removing excess ROS under stress, mainly via the action of SOD, POD, CAT, ascorbyl peroxidase, glutathione reductase and other enzymes (Hussain et al. 2020). SOD is the main oxygen radical scavenger and establishes the first line of defense against ROS in cells, and its enzymatic action leads to the formation of H_2O_2 and O_2 (Alscher et al. 2002). The resulting H_2O_2 is catalyzed by CAT and is decomposed into H_2O and O_2, thereby reducing ROS levels (Raza et al. 2021). In our study, CAT activity of *G. divaricata* under NaCl stress increased significantly at all concentrations, SOD activity only increased significantly at 300 mM, and POD activity gradually increased as salt concentration increased, with both factors being strongly and positively correlated.

MDA content of both salt-tolerant and salt-sensitive varieties of sesame (*Sesamum indicum* L.) seeds increased significantly under 150 mM NaCl treatment (Zhang et al. 2019). In our study, the increase in MDA content under salt stress indicates that plant cells suffer oxidative damage, and the increase in antioxidant enzyme activity suggests that plants eliminated ROS by activating antioxidant enzymes to take defensive measures to reduce oxidative damage. Our results were similar to those of previous studies on the physiological responses of danshen (*Salvia miltiorrhiza*) under salt stress (Xiong et al. 2020). Five concentration gradients (0, 50, 100, 200, 300 mM) of NaCl salt stress also led to an increase in MDA content in danshen roots (Yu et al. 2021). In our study, MDA content in *G. divaricata* leaves increased to varying degrees in response to the NaCl treatments, peaking at 200−400 mM, indicating that these concentrations caused oxidative damage.

When plants are subjected to external stress, they osmoregulate by storing organic substances such as soluble proteins or sugars, amino acids and their derivatives, such as proline, and accumulate organic osmoregulatory substances, allowing cells to absorb water normally and maintain normal growth and development (McNamara and Faria 2012; Faria et al. 2017). Water-soluble proline, which is the main component of plant proteins, enhances the solubility of hydrophobic substances in water, and when plants are stressed, proline participates in their osmomodulation, enhancing their tolerance to osmotic stress, and leading to the accumulation of proline (Srinivas and Balasubramanian 1995). In general, a high proline content in plants under salt stress reflects their stronger stress resistance (Pereira et al. 2021). Kiwi fruit (*Actinidia* sp.) displayed an increase in proline content and a decrease in soluble sugar content under high salt (0.3−0.6% NaCl) concentrations for 15 d (Abid et al. 2020). The soluble sugar content of oats (*Avena sativa* L.) at different growth stages under salt stress (25−50 mM NaCl) showed different trends, with increasing salt content leading to a decrease in soluble sugar content at the heading period, but an increase at the jointing and pustulation stages (Bai et al. 2013). The proline content of *G. divaricata* gradually increased as NaCl stress increased, especially at high concentrations, and proline content and NaCl concentration were strongly and positively correlated. Depending on the NaCl concentration, the soluble sugar content of *G. divaricata*, which was positively correlated with NaCl concentrations, decreased. Therefore, additional research that assesses in greater detail the regulatory effect of soluble sugar on *G. divaricata* salt stress is merited. Another osmoregulatory strategy involves the storage of inorganic ions such as K^+, Na^+, and Cl^-. The main harmful ion caused by salt stress is Na^+, which antagonizes the absorption of other cations in plants and results in a nutritional imbalance (Tester and Davenport 2003; Ashrafi et al. 2018). The ionic radius and hydrophilic capacity of K^+ and Na^+ are similar, so the inhibition of K^+ absorption is more pronounced (Benito et al. 2014). Ionic homeostasis is achieved by maintaining Na^+ / K^+, which is often used as an indicator of salt tolerance (Chhipa and Lal 1995). K^+ is one of the main osmotic solutes in leaves, and when the cytosolic Na^+ / K^+ ratio increases significantly due to K^+ overflow in saline-alkali environments, the normal function of cell membranes becomes impaired, which in turn affects metabolism and the physiological functions of the entire cell (Roman et al. 2020). Under salinity-alkali stress, the Na^+ content in the roots, stems and leaves of fourwing saltbush (*Atriplex canescens* (Pursh) Nutt.) increased while K^+ content remained relatively stable or decreased, while the disturbance of Na^+ / K^+ balance and the concomitant decrease in photosynthetic ability led to inhibited seedling growth (Zhang et al. 2019). In pea (*Pisum sativum* L.), as salt (0−75 mM NaCl) concentration increased to 75 mM, Na^+ content in roots and stems increased and Na^+ / K^+ became elevated, which may have impacted photosynthesis (Shahid et al. 2012). Mg^{2+} is an essential nutrient for plant growth and one of the molecular components of synthetic chlorophyll, and some enzymes in photosynthesis must also be activated by the action of Mg^{2+} (Li et al. 2010). High concentrations of Na^+ replaced Mg^{2+} in cell membranes, and increasing Na^+ concentration decreased Mg^{2+} ion activity, resulting in a decrease in Mg^{2+} content in alfalfa (*Medicago sativa* L.) extracts (Li et al. 2010). The concentration of Mg^{2+} in pepper (*Capsicum annuum* L.) leaves decreased in 60 mM NaCl and 60 mM KCl treatments (Martínez-Ballesta et al. 2004). In our study, Na^+ increased significantly in *G. divaricata* leaves, especially at 200 mM NaCl, and an opposite trend in K^+ content was observed between 200−400 mM, Na^+/K^+ peaked at 200 mM, and when NaCl concentration was less than 200 mM, Mg^{2+} content remained stable, decreasing significantly at 300−400 mM NaCl. Cumulatively, this indicates that *G. divaricata* was severely negatively impacted by Na^+ during NaCl stress, stimulating the absorption of Mg^{2+}. In this study, when NaCl concentration exceeded 200 mM, *G. divaricata* could not develop normal roots, and most of the growth and physiological indicators showed significantly lower values above 200 mM, indicating the negative impact of salinity stress on these essential functions. Therefore, the maximum tolerated NaCl concentration in *ex vivo* culture was 200 mM. Halophytes can grow and complete their life cycle in habitats where salt concentration exceeds 200 mM NaCl (Flowers et al. 1986). *G. divaricata*

has a certain degree of NaCl tolerance, but is not classified as a halophyte, but can grow in environments with a certain degree of salinization, and is also suitable for improving soil salinization and restoration of island vegetation.

Function and regulatory mechanism

The growth characteristics and physiological and biochemical responses of *G. divaricata* under salt stress were previously reported (Wang et al. 2017), but the lack of a reference genome for this plant limits the extent of molecular studies of the salt tolerance mechanism. Transcriptome sequencing is an important tool for studying gene expression in stressful environments, providing possibilities for the study of functional genes of species without a reference genome. Transcriptome-level sequencing of *G. divaricata* tissue-cultured plantlets under NaCl stress allowed us to quickly screen genes and related metabolic pathways of *G. divaricata* in response to NaCl stress. This information will be helpful for analyzing the function and regulatory mechanism of DEGs in *G. divaricata* under NaCl stress. Lipids, important components of cell structure and function, play an important role as signaling molecules. In addition, lipids can be selectively recovered and catabolized to produce energy during plant development and in response to environmental stresses (Barros et al. 2020). In this study, DEGs identified during GO enrichment analysis showed that the L50 vs control comparison had a large number of DEGs related to lipid metabolism, cellular lipid metabolism and lipid biosynthesis, indicating that there was active lipid metabolism, potentially as a source of energy for the growth and development of *G. divaricata* under low-concentration NaCl stress.

Most DEGs of *G. divaricata* in response to NaCl stress that were significantly enriched were related to plant hormone signaling, MAPK signaling pathway-plant, and starch and sucrose metabolism pathways. Similar pathways were enriched in transcriptional sequencing of wheat (*Triticum aestivum* L.) and morningstar lily (*Lilium pumilum* DC) under salt stress (Amirbakhtiar et al. 2021; Sun et al. 2023).

Hormone signaling

Plant hormone signaling as a central regulator induces changes in gene expression in response to salt. Genes related to plant hormone signaling pathways have been shown to be involved in a variety of plant responses to different levels (0, 150 mM, and 300 mM NaCl) of salt stress, such as orange (*Citrus junos* Siebold ex Yu. Tanaka) (Xie et al. 2018). The signaling cascade composed of an abscisic acid receptor (PYL), protein phosphatase (PP2Cs) and SnRK2s form the core of the abscisic acid (ABA) signaling pathway, ABA accumulation activated PYL while ABA receptor inhibited PP2Cs, PP2C inhibition further induced SnRK2 autophosphorylation, and SnRK2s mediated the ABA reaction through phosphorylation of downstream targets (Ng et al. 2014). The expression of six *StPP2C* genes in potato (*Solanum tuberosum* L.) was upregulated under 200 mM treatment (Wang et al. 2020). *Arabidopsis thaliana* AtPP2CG1 positively regulated salt stress in an ABA-dependent manner, and its overexpression enhanced salt (250 mM NaCl) tolerance, and its loss of function reduced salt tolerance (Liu et al. 2012). PP2C (OsPP108) in rice (*Oryza sativa* L.) was highly induced under ABA (50 µM), salt (300 mM NaCl) and drought stress, and OsPP108 overexpression improved the tolerance of transgenic *A. thaliana* to salt stress, indicating that OsPP108 negatively regulates ABA signaling and positively regulates abiotic stress signals (Singh et al. 2015). BdPP2CA6 of purple falsebrome (*Brachypodium distachyon* L. P. Beauv.) played a positive regulatory role in both the ABA signaling pathway and the response to salt stress when 100 µM ABA, 200 mM NaCl, or 20% PEG-6000 were used (Zhang et al. 2017). In this study, the expression of four PP2C genes in *G. divaricata* leaves was upregulated under NaCl stress (Fig. 13a). There was an interaction between plant hormones, in which the key protein kinase SnRK2s of the ABA signaling pathway interacted with the negative regulator of cytokinin signaling type A recombinant *A. thaliana* two-component response regulator (ARR5) and phosphorylated ARR5 to positively regulate its protein stability (Fig. 10). SnRK2s were inhibited by B-type ARR1, ARR11, and ARR12 in the cytokinin signaling pathway, thereby negatively regulating ABA signaling (Huang et al. 2018). B-type ARRs, together with cytokinin response factors (CRFs), regulate the transcription of cytokinin primary response genes, including type A ARRs (To et al. 2004). Auxin plays a key role in most plant growth responses, and the auxin-responsive factor (ARF) family plays a key role in regulating the expression of auxin-responsive genes (Li et al. 2016a). AUX/IAA at the C-terminus of the ARF protein formed a heterodimer with indole-3-acetic acid, which functions as an auxin (Ulmasov et al. 1999). The expression of ARF-38 and MaARF2 in banana (*Musa nana* Lour.) was upregulated under salt stress (200 mM mannitol or 300 mM NaCl), indicating that they may be involved in the regulation of the response to salt stress and could be used as candidate genes for stress resistance breeding (Hu et al. 2015b; Huang 2020). In addition, *A. thaliana* ARF2 was shown to bind to the K^+ transporter gene HAK5 promoter region and regulate K^+ metabolic balance (Zhao et al. 2016). GmTGA17 of soybean (*Glycine max* L.) and MhTGA2 of apple (*Malus hupehensis* Pamp. Rehder) had positive regulatory effects on these plants' responses to salt (200 mM NaCl) stress (Du et al. 2014; Li et al. 2019). Under salt stress, the expression of A-ARR in the cytokinin signaling pathway and ARF expression in the auxin signaling pathway were upregulated (Fig. 13a). In addition, GID in the gibberellin pathway and TGA in the SA pathway were also associated with the response of *G. divaricata* to salt stress (Fig. 10). In conclusion, there are complex cross-interactions between different plant hormones to jointly regulate a plant's response to salt stress.

The MAPK cascade is mainly composed of three subfamilies, namely mitogen-activated protein kinase (MAPKKK), mitogen-activated protein kinase (MAPKK) and mitogen-activated protein kinase (MAPK), which play an important role in signal transduction of biotic and abiotic stress in plants (Ma et al. 2022). OsMKK1, OsMPK4, OsMKK6, OsMAPKKK63, and others constitute signaling transduction pathways that regulate salt tolerance (130–200 mM NaCl) in rice (Wang et al. 2014) and salt tolerance (175 mM NaCl) in *A. thaliana* (Na et al. 2019). The MAPK cascade (MEKK1-MKK1/MKK2-MPK4) is a key regulator of ROS and SA accumulation and plays a central role in oxidative stress signaling (Pitzschke et al. 2009). The MAPK activity of Canada mint (*Mentha canadensis* L.) increased significantly under 150 mM NaCl stress, which enhanced the expression of V^-H^+-ATPase, thereby maintaining ionic homeostasis in cells (Li et al. 2016). The DEGs in the MAPK signaling pathway of *G. divaricata* under NaCl stress may be related to antioxidant processes and ion balance. MAPK is associated with hormones, ROS and other signaling molecules, and a large number of studies have shown that auxin, ABA, ethylene, jasmonic acid, other hormones and H_2O_2 can induce MAPK activity (Mishra et al. 2006; Rodriguez et al. 2010). *A. thaliana* AP2C1 (B-type PP2C) inactivated MPK4 and MPK6, thereby regulating hormone levels and defense responses (Schweighofer et al. 2007). In our study, nine DEGs simultaneously mediated two pathways of plant hormone signaling and the MAPK pathway, including four PP2C genes and one ERF1 gene that were up-regulated (Fig. 11).

Osmotic stress signaling

Sucrose is the main form of carbohydrate transport, providing energy for plant growth and development (Sturm et al. 1999). With the extension of salt stress over time, the damage to plants increases, and a large number of soluble carbohydrates can be produced during starch and sucrose metabolism, which could neutralize the harm caused by osmotic stress under salt stress. Other studies have shown that there were interactions between starch and sucrose metabolic pathways and plant hormone signaling pathways to jointly regulate and control plant growth and development processes (Liu et al. 2018; Chen et al. 2023). Under NaCl stress, the expression of three invertase (INV) genes and two sucrose synthase (SUS) genes in the metabolic pathways of starch and soluble sugar in *G. divaricata* was upregulated (Fig. 13c). Both SUS and INV can catalyze the decomposition of sucrose, and the reaction in which SUS participates is reversible and mainly synthesizes sucrose, while INV irreversibly hydrolyzes sucrose to produce glucose and fructose, providing plants with a carbon backbone and energy (Sturm 1999). The expression of PtCWINV4, PtVINV1/2 and PtVINV3 in the leaves of populus (*Populus tomentosa* Carrière) under salt treatment (400 mM NaCl) was upregulated, and the expression of *PtVINV1/2* in roots was upregulated (Chen et al. 2015). The SUS gene of watermelon (*Citrullus lanatus* Thunb.) was upregulated under salt stress (150 mM NaCl), thereby increasing sucrose content, maintaining plant cell metabolism, and enhancing plant salt tolerance (Liu et al. 2023).

Ionic stress signaling

Plant roots absorb large amounts of Na^+ and Cl^- in high-salt environments, causing ion toxicity, and transporters play a key role in ion absorption, transport and chelation. Plants maintain the balance of cell ions through different Na^+ transporters, thereby ensuring normal plant growth (Horie et al. 2009; Xu et al. 2021). Plant high-affinity K^+ transporter (HKT) has been widely studied and plays a key role in Na^+ and K^+ balance in salt stress and is an important component of plant salt tolerance (Platten et al. 2006). Increased expression of HKT limited the transport of Na^+ to the aboveground organs and maintained low Na^+ / K^+ to improve the tolerance of *A. thaliana* to salt (50 mM NaCl) (Tada 2019) and also cotton to salt (250 mM NaCl) (Guo et al. 2020). HKT genes were expressed in response to Na^+ and K^+ concentrations, but did not follow a specific trend associated with the concentration of plant ions, and some HKT genes were upregulated at a high Na^+ concentration (150 mM NaCl) in Chinese licorice (*Glycyrrhiza inflata* Batalin) (Xu et al. 2021), while some HKT genes were downregulated (Golldack et al. 2002; Ali et al. 2016; Dave et al. 2022). In this study, the expression of cationic transporter (TRK, HKT) in *G. divaricata* was downregulated under salt stress (Fig. 13). Potassium transport protein (KUP), another transporter that can mediate high-affinity potassium uptake, and belonging to the potassium-hydrogen ion co-transporter family HAK/KUP/KT, was strongly induced to mediate plant K^+ uptake under low potassium stress (Kim et al. 1998; Grabov 2007). The expression of KUP in *G. divaricata* leaves under salt stress was upregulated (Fig. 13d), indicating that potassium ions absorbed by *G. divaricata* under salt stress mainly relied on KUP rather than HKT. In addition, the expression of magnesium ion transporters (MRS2, MFM1) in *G. divaricata* leaves was upregulated (Fig. 13d). The MRS2 protein family plays a major role in Mg^{2+} transport, and *A. thaliana* AtMRS2-11 formed an Mg^{2+} channel that mediated rapid Mg^{2+} transport in the absence of additional protein chaperones (Schock 2000; Ishijima 2021).

Existing studies have shown that multiple TFs are involved in regulating changes in gene expression under salt stress. Most of the salt-response genes of *Populus davidiana* × *P. bolleana* belong to the ERF, MYB, WRKY, NAC, and bHLH TF families (Lei et al. 2022). An analysis of TF-encoding DEGs in *G. divaricata* under salt stress mainly annotated MYB, AP2/ERF, bHLH, NAC, and C2C2 TF families, mostly MYB (Fig. 14). Many studies reported the important role of the MYB gene in plants' tolerance to salt (Tang et al. 2019; Bian et al. 2020). MYB promoted keratin and lignin formation, increased Ca^{2+} levels, and upregulate the transcription of POX and LEA, thereby enhancing plant salt tolerance (Wu et al. 2019; Zhang et al. 2020). The AP2/ERF family is a large family of plant-specific TFs with a highly conserved DNA-binding domain that plays important regulatory roles in many biological and physiological processes, such as plant morphogenesis, response mechanisms to various stresses, hormone signaling, and metabolite regulation (Feng et al. 2020). The AP2/ERF family included dehydration reactor binding (DREB), found in *A. thaliana* and alfalfa (*Medicago sativa* L.), increasing tolerance to salt stress in DREB-overexpressing plants (Kasuga et al. 1999; Jin et al. 2010). OrbHLH2 in *A. thaliana* functions upstream of DREB1/CBF3, which in turn bind to CRE/DRE elements in RD29A and KIN1 genes, thereby increase tolerance to salt stress (Zhou et al. 2009). MYC2 is a bHLH TF that mediates the activation of MYC2 under salt stress and regulates the biosynthesis of proline, thereby regulating salt stress. NAC TFs also play an important role in plant stress responses (Verma et al. 2020). *OsNAC022* enhanced the tolerance of transgenic rice plants to salt stress by modulating ABA-mediated pathways (Hong et al. 2016). More research on the mechanisms of salt tolerance in plants is needed to identify key roles in transcriptional regulation and to systematically understand salt stress responses (Seki et al. 2002).

Conclusion

Growth indicators, antioxidant enzyme activity, and MDA, proline, and soluble sugar content were determined in the leaves of *G. divaricata* exposed to 0, 50 and 200 mM NaCl to explore the mechanism of NaCl tolerance at the transcriptome level, identifying several key biological pathways and candidate genes associated with the response to NaCl. In the plant hormone signaling pathway, PP2Cs of the ABA pathway, ARF in the auxin pathway, CRE1 in the cytokinin pathway, GID1 in the A-ARR and gibberellin pathway, and TGA in SA pathway were involved in the regulation of several biochemical pathways under NaCl stress. In addition, four upregulated PP2Cs in the plant hormone signaling pathway and one upregulated ERF1 in the MAPK signaling pathway were identified, suggesting cross-talk or interaction between these biological pathways. SUS and INV expression was upregulated in salt stress, and may be another key response to enhancing salt tolerance in *G. divaricata*. The expression of cation and sodium-related transporters related to sodium ion transport were down-regulated, while the expression of potassium ion transporter and magnesium ion transporter (MRS2, MFM1) was upregulated, indicating that the leaves restricted Na^+ transport and enhanced the transport of K^+ and Mg^{2+} under salt stress. The regulation of TFs such as MYB, AP2/ERF, bHLH, NAC, and C2C2 under NaCl stress was another key strategy in the adaptation to NaCl stress. Based on a transcriptomic analysis, this study revealed a complex NaCl tolerance mechanism of *G. divaricata*, laying a foundation for screening and cloning the key genes related to NaCl tolerance and studying gene interactions, which is of importance for exploring the molecular basis of this phenomenon and for breeding NaCl-tolerant varieties.

Declarations

Ethics Approval and Consent to Participate: Not applicable.

Consent for Publication: Not applicable.

Conflict of interest: The authors declare no competing interests.

References

1. Abid M, Zhang YJ, Li Z, et al. Effect of salt stress on growth, physiological and biochemical characters of four kiwifruit genotypes. Scientia Horticulturae 2020, 271, 109473.
2. Ali A, Raddatz N, Aman R, et al. A single amino-acid substitution in the sodium transporter HKT1 associated with plant salt tolerance. Plant Physiology 2016, 171, 2112−2126.
3. Alscher R G, Erturk N, Heath L S. Role of superoxide dismutases (SODs) in controlling oxidative stress in plants. Journal of Experimental Botany 2002, 53, 1331−1341.
4. Amirbakhtiar N, Ismaili A, Ghaffari M R, et al. Transcriptome analysis of bread wheat leaves in response to salt stress. PLOS One 2021, 16, e0254189.
5. Ashrafi E, Razmjoo J, Zahedi M. Effect of salt stress on growth and ion accumulation of alfalfa (*Medicago sativa* L.) cultivars. Journal of Plant Nutrition 2018, 41, 818−831.
6. Bai JH, Liu JH, Zhang N, et al. Effect of alkali stress on soluble sugar, antioxidant enzymes and yield of oat. Journal of Integrative Agriculture 2013, 12, 1441−1449.
7. Barros JAS, Siqueira JAB, Cavalcanti JHF, et al. Multifaceted roles of plant autophagy in lipid and energy metabolism. Trends in Plant Science 2020, 25, 1141−1153.
8. Benito B, Haro R, Amtmann A, et al. The twins K^+ and Na^+ in plants. Journal of Plant Physiology 2014, 171, 723-731.
9. Bian SM, Jin DH, Sun GQ, et al. Characterization of the soybean R2R3-MYB transcription factor GmMYB81 and its functional roles under abiotic stresses. Gene 2020, 753, 144803.
10. Butcher K, Wick AF, Desutter T, et al. Soil salinity: A threat to global food security. Agronomy Journal 2016, 108, 2189−2200.
11. Chen J, Mangelinckx S, Ma L, et al. Caffeoylquinic acid derivatives isolated from the aerial parts of *Gynura divaricata* and their yeast alpha-glucosidase and PTP1B inhibitory activity. Fitoterapia 2014, 99, 1−6.
12. Chen LF, Meng Y, Bai Y, et al. Starch and sucrose metabolism and plant hormone signaling pathways play crucial roles in *Aquilegia* salt stress adaption. International Journal of Molecular Sciences 2023, 24, 3948.
13. Chen MX, Zhu FY, Wang FZ, et al. Alternative splicing and translation play important roles in hypoxic germination in rice. Journal of Experimental Botany 2019, 70, 817−833.
14. Chen Z, Gao K, Su XX, et al. Genome-wide identification of the invertase gene family in *Populus*. PLOS ONE 2015, 10, e0138540.
15. Chhipa BR & Lal P. Na^+/K^+ ratio as the basis of salt tolerance in wheat. Australian Journal of Agricultural Research 1995, 46.533−539.
16. Chou SC, Chuang LM, Lee SS. Hypoglycemic constituents of *Gynura divaricata* subsp. *formosana*. Natural Product Communications 2012, 7, 221−222.
17. Chourasia KN, Lal MK, Tiwari RK, et al. Salinity stress in potato: Understanding physiological, biochemical and molecular responses. Life (Basel) 2021, 11, 545.
18. Dave A, Agarwal P, Agarwal PK. Mechanism of high affinity potassium transporter (HKT) towards improved crop productivity in saline agricultural lands. 3 Biotech 2022, 12, 51.
19. Derakhshani Z, Bhave M, Shah RM. Metabolic contribution to salinity stress response in grains of two barley cultivars with contrasting salt tolerance. Environmental and Experimental Botany 2020, 179, 104229.
20. Du X, Du B, Chen X, et al. Overexpression of the *MhTGA2* gene from crab apple (*Malus hupehensis*) confers increased tolerance to salt stress in transgenic apple (*Malus domestica*). The Journal of Agricultural Science 2014, 152, 634−641.
21. Eden E, Navon R, Steinfeld I, Lipson D, Yakhini Z. Gorilla: a tool for discovery and visualization of enriched GO terms in ranked gene lists. BMC Bioinformatics 2009, 10, 48.
22. Faria SC, Provete DB, Thurman CL, McNamara JC. Phylogenetic patterns and the adaptive evolution of osmoregulation in fiddler crabs (Brachyura, Uca). PLoS ONE 2017, 12, e0171870.
23. Farooq M, Ahmad R, Shahzad M, et al. Differential variations in total flavonoid content and antioxidant enzymes activities in pea under different salt and drought stresses. Scientia Horticulturae 2021, 287, 110258.
24. Feng XH, Hussain T, Guo K, et al. Physiological, morphological and anatomical responses of *Hibiscus moscheutos* to non-uniform salinity stress. Environmental and Experimental Botany 2021, 182, 104301.

25. Flora of China Editorial Committee. Chinese Academy of Sciences. Flora of China. Beijing: Science Press 1999, 77, 317.

26. Flowers TJ, Hajibagheri MA, Clipson NJW. Halophytes. The Quarterly Review of Biology 1986, 61, 313–337.

27. Frukh A, Siddiqi TO, Khan MIR, et al. Modulation in growth, biochemical attributes and proteome profile of rice cultivars under salt stress. Plant Physiology and Biochemistry 2020, 146, 55–70.

28. Golldack D, Su H, Quigley F, et al. Characterization of a HKT-type transporter in rice as a general alkali cation transporter. The Plant Journal 2002, 31, 529–542.

29. Grabov A. Plant KT/KUP/HAK potassium transporters: single family-multiple functions. Annals of Botany 2007, 99, 1035–1041

30. Gu LJ, Wang HT, Wei HL, et al. Identification, expression, and functional analysis of the group iid WRKY subfamily in upland cotton (*Gossypium hirsutum* L.). Frontiers in Plant Science, 2018, 9, 1684.

31. Guo Q, Meng S, Tao SC, et al. Overexpression of a samphire high-affinity potassium transporter gene *SbHKT1* enhances salt tolerance in transgenic cotton. Acta Physiologiae Plantarum 2020, 42, 36.

32. Hong YB, Zhang HJ, Huang L, et al. Overexpression of a stress-responsive NAC transcription factor gene *ONAC022* improves drought and salt tolerance in rice. Frontiers in Plant Science 2016, 7, 4.

33. Horie T, Hauser F, Schroeder J I. HKT transporter-mediated salinity resistance mechanisms in *Arabidopsis* and monocot crop plants. Trends in Plant Science 2009, 14, 660–668.

34. Hu LX, Li HY, Chen L, et al. RNA-seq for gene identification and transcript profiling in relation to root growth of bermudagrass (*Cynodon dactylon*) under salinity stress. BMC Genomics 2015a, 16, 575.

35. Hu W, Zuo J, Hou XW, et al. The auxin response factor gene family in banana: genome-wide identification and expression analyses during development, ripening, and abiotic stress. Frontiers in Plant Science 2015b, 6, 742.

36. Huang DM, Xu Y, Wu B, et al. Cloning and sequence expression analysis of banana *MaARF2* gene. Journal of Tropical Crops 2020, 41, 89–96.

37. Huang XZ, Hou LY, Meng JJ, et al. The antagonistic action of abscisic acid and cytokinin signaling mediates drought stress response in *Arabidopsis*. Molecular Plant 2018, 11, 970–982.

38. Hussain MI, Elnaggar A, El-Keblawy A. Eco-physiological adaptations of *Salsola drummondii* to soil salinity: Role of reactive oxygen species, ion homeostasis, carbon isotope signatures and anti-oxidant feedback. Plant Biosystems 2020, 155, 1133–1145.

39. Ishijima S, Shiomi R, Sagami I. Functional analysis of whether the glycine residue of the GMN motif of the *Arabidopsis* MRS2/MGT/CorA-type Mg^{2+} channel protein AtMRS2-11 is critical for Mg^{2+} transport activity. Archives of Biochemistry and Biophysics 2021, 697, 108673.

40. Jin TC, Chang Q, Li WF, et al. Stress-inducible expression of *GmDREB1* conferred salt tolerance in transgenic alfalfa. Plant Cell, Tissue and Organ Culture 2010 100, 219–227.

41. Kim EJ, Kwak JM, Uozumi N, et al. *AtKUP1*: an *Arabidopsis* gene encoding high-affinity potassium transport activity. The Plant Cell 1998, 10, 51–62.

42. Kulak M, Gul F, Sekeroglu N. Changes in growth parameter and essential oil composition of sage (*Salvia officinalis* L.) leaves in response to various salt stresses. Industrial Crops and Products 2020, 145, 112078.

43. Kurban H, Saneoka H, Nehira K, et al. Effect of salinity on growth, photosynthesis and mineral composition in leguminous plant *Alhagi pseudoalhagi* (Bieb.). Soil Science and Plant Nutrition 1999, 45, 851–862.

44. Lei XJ, Liu ZY, Xie QJ, et al. Construction of two regulatory networks related to salt stress and lignocellulosic synthesis under salt stress based on a *Populus davidiana × P. bolleana* transcriptome analysis. Plant Molecular Biology 2022, 109, 689–702.

45. Li B, Liu Y, Cui XY, et al. Genome-wide characterization and expression analysis of soybean TGA transcription factors identified a novel TGA gene involved in drought and salt tolerance. Frontiers in Plant Science 2019, 10, 549.

46. Li BB, Ding Y, Tang XL, et al. Effect of L-arginine on maintaining storage quality of the white button mushroom (*Agaricus bisporus*). Food and Bioprocess Technology 2019, 12, 563–574.

47. Li PC, Yang XY, Wang HM, et al. Metabolic responses to combined water deficit and salt stress in maize primary roots. Journal of Integrative Agriculture 2021, 20, 109–119.

48. Li RL, Shi FC, Fukuda K, et al. Effects of salt and alkali stresses on germination, growth, photosynthesis and ion accumulation in alfalfa (*Medicago sativa* L.). Soil Science and Plant Nutrition 2010, 56, 725–733.

49. Li SB, Xie ZZ, Hu CG, et al. A review of auxin response factors (*ARFs*) in plants. Frontiers in Plant Science 2016a, 7, 47.

50. Li WL, Ren BR, Min Z, et al. The anti-hyperglycemic effect of plants in genus *Gynura* Cass. The American Journal of Chinese Medicine 2009, 37, 961–966.

51. Li XY, Liu DM, Wang J, et al. Morphological, biochemical and physiological responses of a tropical coastal plant *Guettarda speciosa* to salt stress. Global Ecology and Conservation 2021, 32, e01887.

52. Li Z, Zhen Z, Guo K, et al. MAPK-mediated enhanced expression of vacuolar H^+-ATPase confers the improved adaption to NaCl stress in a halotolerate peppermint (*Mentha piperita* L.). Protoplasma 2016, 253, 553–569.

53. Liang MT, Hu F, Xie DS, et al. Physiological measurements and transcriptome survey reveal how semi-mangrove *Clerodendrum inerme* tolerates saline adversity. Frontiers in Plant Science 2022, 13, 882884.

54. Liu C, Chen X, Ma PA, et al. Ethylene responsive factor MeERF72 negatively regulates *sucrose synthase 1* gene in cassava. International Journal of Molecular Sciences 2018, 19, 1281.

55. Liu X, Zhu YM, Zhai H, et al. *AtPP2CG1*, a protein phosphatase 2C, positively regulates salt tolerance of *Arabidopsis* in abscisic acid-dependent manner. Biochemical and Biophysical Research Communications 2012, 422, 710–715.

56. Liu Y, Zhang W-H, Elango D, et al. Metabolome and transcriptome analysis reveals molecular mechanisms of watermelon under salt stress. Environmental and Experimental Botany 2023, 206, 105200.

57. Livak KJ, Schmittgen TD. Analysis of relative gene expression data using realtime quantitative PCR and the $2^{-\Delta\Delta CT}$ method. Methods 2001, 25, 402−408.

58. Machado RMA, Serralheiro RP. Soil salinity: Effect on vegetable crop growth. Management practices to prevent and mitigate soil salinization. Horticulturae 2017, 3, 30.

59. Ma H, Gao Y, Wang Y, Dai Y, Ma H. Regulatory mechanisms of mitogen-activated protein kinase cascades in plants: more than sequential phosphorylation. Int. J. Mol. Sci. 2022, 23, 3572.

60. Mao XZ, Cai T, Olyarchuk JG, Wei LP. Automated genome annotation and pathway identification using the KEGG Orthology (KO) as a controlled vocabulary. Bioinformatics 2005, 21, 3787−3793.

61. Martínez-Ballesta MC, Martínez V, Carvajal M. Osmotic adjustment, water relations and gas exchange in pepper plants grown under NaCl or KCl. Environmental and Experimental Botany 2004, 52, 161−174.

62. McNamara JC, Faria SC. Evolution of osmoregulatory patterns and gill ion transport mechanisms in the decapod Crustacea: a review. J Comp Physiol. 2012, 182B: 997−1014.

63. Mishra NS, Tuteja R, Tuteja N. Signaling through MAP kinase networks in plants. Archives of Biochemistry and Biophysics 2006, 452, 55−68.

64. Mittler R, Vanderauwera S, Gollery M, et al. Reactive oxygen gene network of plants. Trends in Plant Science 2004, 9, 490−498.

65. Muchate NS, Nikalje GC, Rajurkar NS, et al. Plant salt stress: Adaptive responses, tolerance mechanism and bioengineering for salt tolerance. The Botanical Review 2016, 82, 371−406.

66. Murashige T, Skoog F. A revised medium for rapid growth and bioassays with tobacco tissue cultures. Physiol Plant 1962, 15, 473−497.

67. Na YJ, Choi HK, Park MY, et al. OsMAPKKK63 is involved in salt stress response and seed dormancy control. Plant Signaling & Behavior 2019, 14, e1578633.

68. Ng LM, Melcher K, Teh BT, et al. Abscisic acid perception and signaling: structural mechanisms and applications. Acta Pharmacologica Sinica 2014, 35, 567−584.

69. Pereira EG, Amaral MB, Bucher CA, Santos LA, Fernandes MS, Rossetto CAV. Proline osmopriming improves the root architecture, nitrogen content and growth of rice seedlings. Biocatalysis and Agricultural Biotechnology 2021, 33,101998,

70. Pitzschke A, Djamei A, Bitton F, et al. A major role of the MEKK1-MKK1/2-MPK4 pathway in ROS signalling. Molecular Plant 2009, 2, 120−137.

71. Platten JD, Cotsaftis O, Berthomieu P, et al. Nomenclature for HKT transporters: key determinants of plant salinity tolerance. Trends in Plant Science 2006, 11, 372−374.

72. Qadir M, Shams M. Some agronomic and physiological aspects of salt tolerance in cotton (*Gossypium hirsutum* L.). Journal of Agronomy and Crop Science 1997, 179, 101−106.

73. Raza A, Su W, Gao A, et al. Catalase (CAT) gene family in rapeseed (*Brassica napus* L.): genome-wide analysis, identification, and expression pattern in response to multiple hormones and abiotic stress conditions. International Journal of Molecular Sciences 2021, 22, 4281.

74. Rodriguez MCS, Petersen M, Mundy J. Mitogen-activated protein kinase signaling in plants. Annual Review of Plant Biology 2010, 61, 621−649.

75. Roman V J, Toom LA, Gamiz CC, et al. Differential responses to salt stress in ion dynamics, growth and seed yield of European quinoa varieties. Environmental and Experimental Botany 2020, 177, 104146.

76. Schock I, Gregan J, Steinhauser S, et al. A member of a novel *Arabidopsis thaliana* gene family of candidate Mg^{2+} ion transporters complements a yeast mitochondrial group II intron-splicing mutant. Plant Journal 2010, 24, 489−501.

77. Schweighofer A, Kazanaviciute V, Scheikl E, et al. The PP2C-type phosphatase AP2C1, which negatively regulates MPK4 and MPK6, modulates innate immunity, jasmonic acid, and ethylene levels in *Arabidopsis*. The Plant Cell 2007, 19, 2213−2224.

78. Seki M, Narusaka M, Ishida J, et al. Monitoring the expression profiles of 7000 *Arabidopsis* genes under drought, cold and high-salinity stresses using a full-length cDNA microarray. The Plant Journal 2002, 31, 279−292.

79. Shahid MA, Balal RM, Pervez MA, et al. Differential response of pea (*Pisum sativum* L.) genotypes to salt stress in relation to the growth, physiological attributes antioxidant activity and organic solutes. Australian Journal of Crop Science 2012, 6, 828−838.

80. Singh, Jha S K, Bagri J, et al. ABA inducible rice protein phosphatase 2C confers ABA insensitivity and abiotic stress tolerance in *Arabidopsis*. Plos ONE 2015, 10, e0125168.

81. Srinivas V, Balasubramanian D. Proline is a protein-compatible hydrotrope. Langmuir 1995, 11: 2830−2833.

82. Sturm A, Tang GQ. The sucrose-cleaving enzymes of plants are crucial for development, growth and carbon partitioning. Trends in Plant Science 1999, 4, 401−407.

83. Sturm A. Invertases. Primary structures, functions, and roles in plant development and sucrose partitioning. Plant Physiology 1999, 121, 1−7.

84. Sun SY, Wang YP, Wang JW, et al. Transcriptome responses to salt stress in roots and leaves of *Lilium pumilum*. Scientia Horticulturae 2023, 309, 111622.

85. Tada Y. The *HKT* transporter gene from *Arabidopsis*, *AtHKT1;1*, is dominantly expressed in shoot vascular tissue and root tips and is mild salt stress-responsive. Plants 2019, 8, 204.

86. Takahashi R, Nishio T, Ichizen N, Takano T. Salt-tolerant reed plants contain lower Na^+ and higher K^+ than salt-sensitive reed plants. Acta Physiologia Plantarum 2007, 29, 431−438.

87. Tang YH, Bao XX, Zhi YL, et al. Overexpression of a MYB family gene, *OsMYB6*, increases drought and salinity stress tolerance in transgenic rice. Frontiers in Plant Science 2019, 10, 168.

88. Tester M and Davenport R. Na⁺ tolerance and Na⁺ transport in higher plants. Annals of Botany, 2003, 91, 503−527.

89. To JPC, Haberer G, Ferreira FJ, et al. Type-A *Arabidopsis* response regulators are partially redundant negative regulators of cytokinin signaling. The Plant Cell 2004, 16, 658−671.

90. Ulmasov T, Hagen G, Guilfoyle TJ. Activation and repression of transcription by auxin-response factors. Proceedings of the National Academy of Sciences USA 1999, 96, 5844−5849.

91. Verma D, Jalmi SK, Bhagat PK, et al. A bHLH transcription factor, MYC2, imparts salt intolerance by regulating proline biosynthesis in *Arabidopsis*. FEBS Journal 2020, 287, 2560−2576.

92. Wan CP, Yu YY, Zhou SR, et al. Isolation and identification of phenolic compounds from *Gynura divaricata* leaves. Pharmacognosy Magazine 2011, 7, 101−108.

93. Wang FZ, Jing W, Zhang WH. The mitogen-activated protein kinase cascade MKK1-MPK4 mediates salt signaling in rice. Plant Science 2014, 227, 181−189.

94. Wang JC, Li BC, Meng YX, et al. Transcriptomic profiling of the salt-stress response in the halophyte *Halogeton glomeratus*. BMC Genomics 2015, 16, 169.

95. Wang L, Qin HY, Xu B, et al. Effects of seawater stress on growth and physiological characteristics of *Gynura divaricata*. Jiangsu Agricultural Sciences 2017, 45, 103−108.

96. Wang YF, Liao YQ, Wang YP, et al. Genome-wide identification and expression analysis of *StPP2C* gene family in response to multiple stresses in potato (*Solarium tuberosum* L.). Journal of Integrative Agriculture 2020, 19, 1609−1624.

97. Wang YN, Liang CZ, Meng ZG, et al. Leveraging *Atriplex hortensis* choline monooxygenase to improve chilling tolerance in cotton. Environmental and Experimental Botany 2019, 162, 364−373.

98. Wang ZQ, Zhang WY, Huang WJ, et al. Salt stress affects the fruit quality of *Lycium ruthenicum* Murr. Industrial Crops and Products 2023, 193, 116240.

99. Wu JD, Jiang YL, Liang YN, et al. Expression of the maize MYB transcription factor ZmMYB3R enhances drought and salt stress tolerance in transgenic plants. Plant Physiology and Biochemistry 2019, 137, 179−188.

100. Xie RJ, Pan XT, Zhang J, et al. Effect of salt-stress on gene expression in citrus roots revealed by RNA-seq. Effect of salt-stress on gene expression in citrus roots revealed by RNA-seq. 2018, 18, 155−173.

101. Xiong Y, Li X, Wang T, Gong Y, Zhang C, Xing K, Qin S. Root exudatesdriven rhizosphere recruitment of the plant growth-promoting rhizobacterium *Bacillus flexus* KLBMP 4941 and its growth-promoting effect on the coastal halophyte *Limonium sinense* under salt stress. Ecotoxicol. Environ. Saf. 2020, 194, 110374.

102. Xiong YP, Liang HZ, Yan HF, et al. NaCl-induced stress: Physiological responses of six halophyte species in *in vitro* and *in vivo* culture. Plant Cell, Tissue and Organ Culture 2019a, 139, 531−546.

103. Xiong YP, Yan HF, Liang HZ, et al. RNA-Seq analysis of *Clerodendrum inerme* (L.) roots in response to salt stress. BMC Genomics 2019b, 20, 724.

104. Xu Y, Lu JH, Zhang JD, et al. Transcriptome revealed the molecular mechanism of *Glycyrrhiza inflata* root to maintain growth and development, absorb and distribute ions under salt stress. BMC Plant Biology 2021, 21, 599.

105. Yang JY, Zheng W, Tian Y, et al. Effects of various mixed salt-alkaline stresses on growth, photosynthesis, and photosynthetic pigment concentrations of *Medicago ruthenica* seedlings. Photosynthetica 2011, 49, 275−284.

106. Yang S, Liu HC. Characteristics and cultivation techniques of *Gynura divaricata*. Guangdong Agricultural Sciences 1998, 5, 16−17.

107. Yin YJ, Chen CJ, Guo SW, et al. The fight against *Panax notoginseng* root-rot disease using Zingiberaceae essential oils as potential weapons. Frontiers in Plant Science 2018, 9, 1346.

108. Yu WC, Yu Y, Wang C, et al. Mechanism by which salt stress induces physiological responses and regulates tanshinone synthesis. Plant Physiology and Biochemistry 2021, 164, 10−20.

109. Zhang F, Wei QH, Shi JC, et al. *Brachypodium distachyon* BdPP2CA6 interacts with BdPYLs and BdSnRK2 and positively regulates salt tolerance in transgenic *Arabidopsis*. Frontiers in Plant Science 2017, 8, 264.

110. Zhang P, Wang RL, Yang XP, et al. The R2R3-MYB transcription factor AtMYB49 modulates salt tolerance in *Arabidopsis* by modulating the cuticle formation and antioxidant defense. Plant, Cell & Environment 2020, 43, 1925−1943.

111. Zhang T, He KN, Zhang ZZ. The effects of salt and alkaline stress on the fourwing saltbush (*Atriplex canescens* (Pursh) Nutt.) stress. Applied Ecology and Environmental Research 2019, 17, 8583−8598.

112. Zhang YJ, Wei MY, Liu AL, et al. Comparative proteomic analysis of two sesame genotypes with contrasting salinity tolerance in response to salt stress. Journal of Proteomics 2019, 201, 73−83.

113. Zhang ZY, Liu HH, Sun C, et al. A C2H2 zinc-finger protein OsZFP213 interacts with OsMAPK3 to enhance salt tolerance in rice. Journal of Plant Physiology 2018, 229, 100−110.

114. Zhao S, Zhang ML, Ma TL, et al. Phosphorylation of ARF2 relieves its repression of transcription of the K⁺ transporter gene *HAK5* in response to low potassium stress. Plant Cell 2016, 28, 3005−3019.

Tables

Table 1 Effects of NaCl stress on growth indicators of *Gynura divaricata*

NaCl concentration (mM)	Rooting (%)			Mortality (%)	Mean root number	Mean root length (cm)	Mean plantlet height (mm)	Mean biomass (mg)	Water content (%)
	7 days	14 days	21 days						
0	98.89 ± 1.11 a	100 ± 0.00 a	100 ± 0.00 a	0 a	5.67 ± 0.35 a	8.12 ± 0.18 a	12.27 ± 0.52 a	198.81 ± 19.79 bc	95.01 ± 0.51 a
50	83.33 ± 1.92 b	98.89 ± 1.11 a	100 ± 0.00 a	0 a	5.07 ± 0.23 ab	8.65 ± 0.23 a	10.03 ± 0.11 b	207.84 ± 5.50 b	95.30 ± 0.22 a
100	28.89 ± 2.22 c	81.11 ± 2.22 b	88.89 ± 2.94 b	0 a	4.40 ± 0.13 b	8.21 ± 0.20 a	9.86 ± 0.17 b	209.25 ± 3.52 ab	94.92 ± 0.56 a
200	0 d	53.33 ± 3.85 c	76.67 ± 3.33 c	0 a	2.80 ± 0.12 c	4.02 ± 0.24 b	8.52 ± 0.14 c	245.89 ± 14.84 a	94.30 ± 0.16 b
300	0 d	0 d	4.44 ± 1.11 d	0 a	1.33 ± 0.33 d	0.68 ± 0.17 c	8.04 ± 0.54 c	219.62 ± 12.16 ab	93.44 ± 0.57 c
400	0 d	0 d	0 d	1.11 ± 1.11 a	0 e	0 d	7.89 ± 0.32 c	170.66 ± 7.40 c	92.48 ± 0.45 d

The results were obtained from three biological replicates for each sample. Different lowercase letters in the table indicate significant differences ($P \leq 0.05$). n = 30 per treatment

Table 2 Correlation analysis between growth and physiological indicators of *Gynura divaricata* under NaCl stress

	NaCl concentration	CAT	POD	SOD	MDA	Proline	Soluble sugar	Na⁺	K⁺	Mg²⁺	Na⁺ / K⁺	Ro nu
NaCl concentration	1											
CAT	-0.114	1										
POD	0.992**	-0.171	1									
SOD	0.533	-0.16	0.519	1								
MDA	0.751	0.174	0.772	0.33	1							
Proline	0.932**	-0.175	0.932**	0.232	0.621	1						
Soluble sugar	-0.923**	-0.054	-0.884*	-0.738	-0.677	-0.748	1					
Na⁺	0.906*	-0.031	0.920**	0.563	0.938**	0.753	-0.853*	1				
K⁺	-0.33	-0.822*	-0.319	-0.005	-0.62	-0.269	0.356	-0.445	1			
Mg²⁺	-0.900*	0.188	-0.859*	-0.534	-0.405	-0.873*	0.879*	-0.65	0.09	1		
Na⁺ / K⁺	0.849*	0.02	0.876*	0.43	0.978**	0.725	-0.754	0.983**	-0.519	-0.538	1	
Root number	-0.999**	0.139	-0.995**	-0.548	-0.752	-0.927**	0.921**	-0.911*	0.313	0.896*	-0.853*	1
Root length	-0.964**	0.31	-0.977**	-0.65	-0.706	-0.864*	0.884*	-0.901*	0.17	0.854*	-0.833*	0.9
Plantlet height	-0.898*	-0.262	-0.883*	-0.553	-0.886*	-0.744	0.912*	-0.936**	0.653	0.700	-0.908*	0.8
Biomass	-0.235	0.232	-0.2	0.221	0.363	-0.487	0.098	0.188	-0.24	0.543	0.248	0.2
Water content	-0.969**	0.321	-0.969**	-0.482	-0.613	-0.954**	0.846*	-0.813*	0.122	0.928**	-0.746	0.9

Three biological replicates and three technical repeats for each sample.** Significant correlation at $P < 0.01$ (double-tailed); * significant correlation at $P < 0.05$ (double-tailed).

Table 3 Statistics of the sequencing data quality of *Gynura divaricata*

Sample	Raw reads	Clean reads	Raw bases (bp)	Clean bases (bp)	Q30 (%)	GC content (%)
CK_1	45261664	44969740	6834511264	6688580066	92.58	43.02
CK_2	47521962	47147558	7175816262	6999922420	93.17	43.53
CK_3	45837324	45523674	6921435924	6765619896	92.68	43.15
L50_1	45155128	44870434	6818424328	6679339329	93.26	43.17
L50_2	58410690	57982988	8820014190	8639699974	93.39	43.52
L50_3	45144860	44862164	6816873860	6672644573	92.89	43.51
L200_1	45832406	45534370	6920693306	6765907493	93.19	42.91
L200_2	52780042	52388006	7969786342	7773882970	93.27	43.43
L200_3	43713484	43405450	6600736084	6460437591	93.51	43.50

The qRT-PCR results were obtained from three biological replicates and three technical repeats for each gene and sample.

Supplementary Tables

Supplementary Tables 2-5 not available with this version.

Figures

Figure 1

Effects of NaCl stress on the growth of *Gynura divaricata*

From left to right, NaCl concentrations were 0, 50, 100, 200, 300 and 400 mM, respectively. a-b, Shoot growth on MS medium with 0.5 mg L^{-1} IBA for 3 wks; c, rooted plantlets within 4 wks; d, changes in the color and size of leaves within 6 wks. Bars = 2 cm.
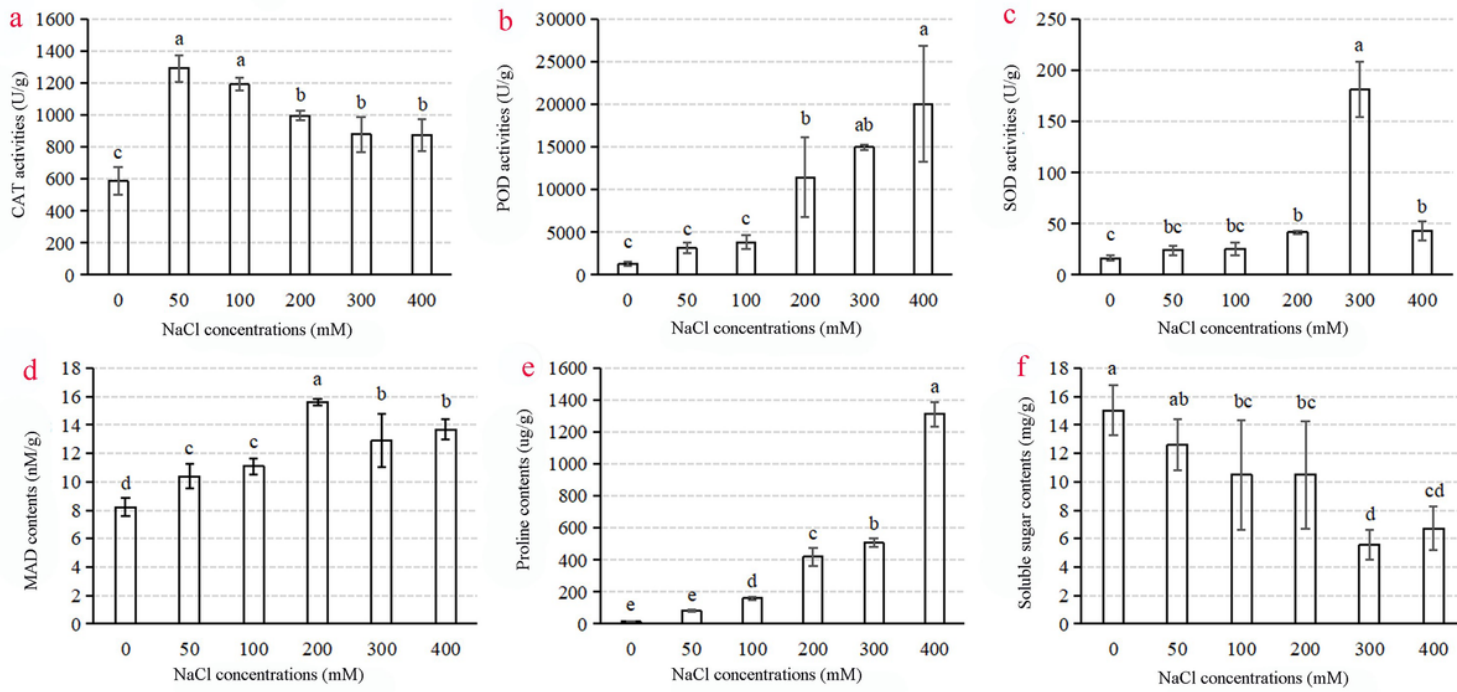
Figure 2

Effects of NaCl stress on antioxidant enzyme activity, MDA content and osmolyte content of *Gynura divaricata*

Different lower-case letters within the SPC column indicate significant differencesaccording to Duncan's multiple range test ($P \leq 0.05$). n = 30 per treatment.
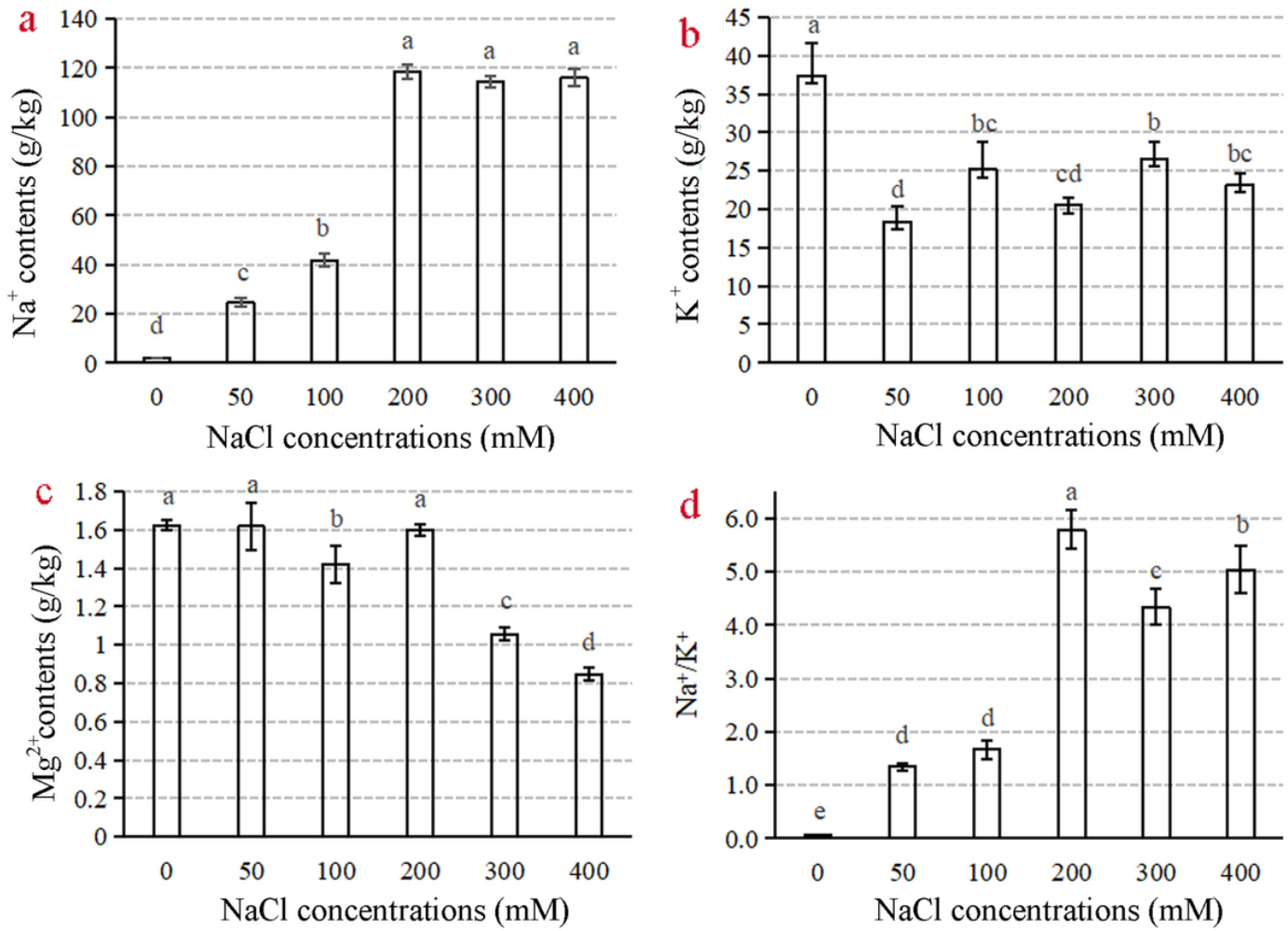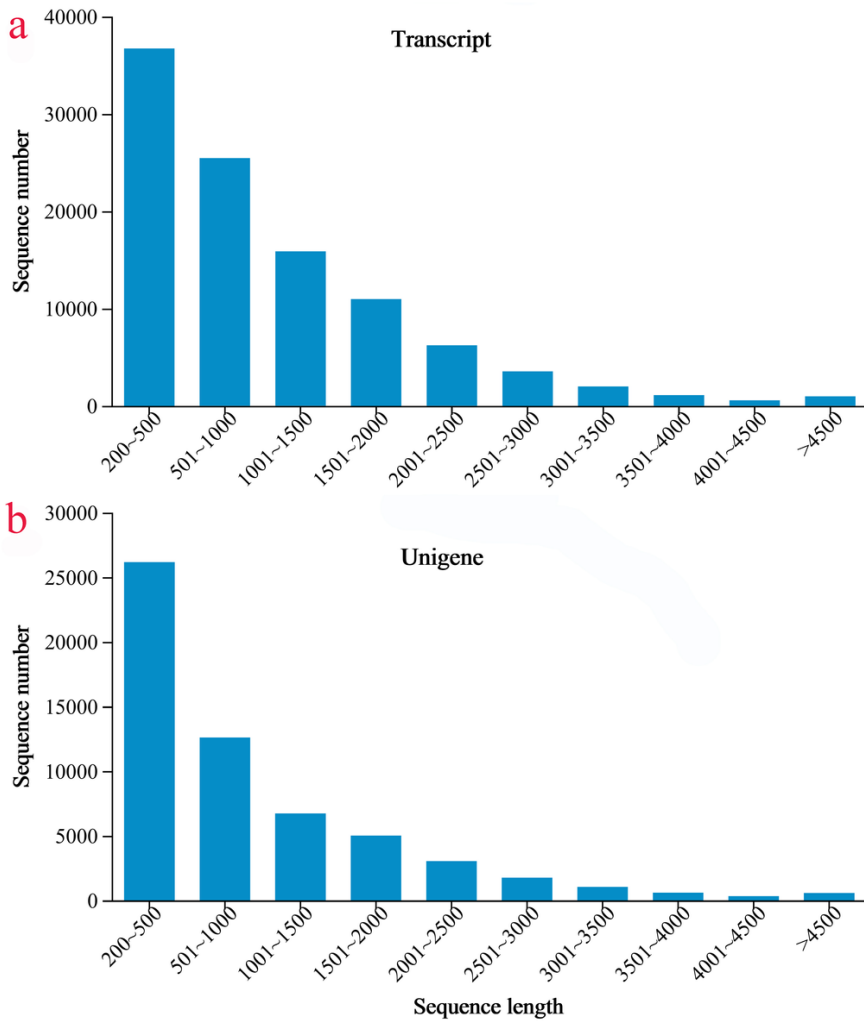
Figure 3

Effects of NaCl stress on the content of Na$^+$, K$^+$, and Mg^{2+} of *Gynura divaricata*

Different lower-case letters within the SPC column indicate significant differences according to Duncan's multiple range test ($P \leq 0.05$. n = 30 per treatment.

Figure 4

Length distribution of transcripts (a) and unigenes (b) of *Gynura divaricata* under NaCl stress.
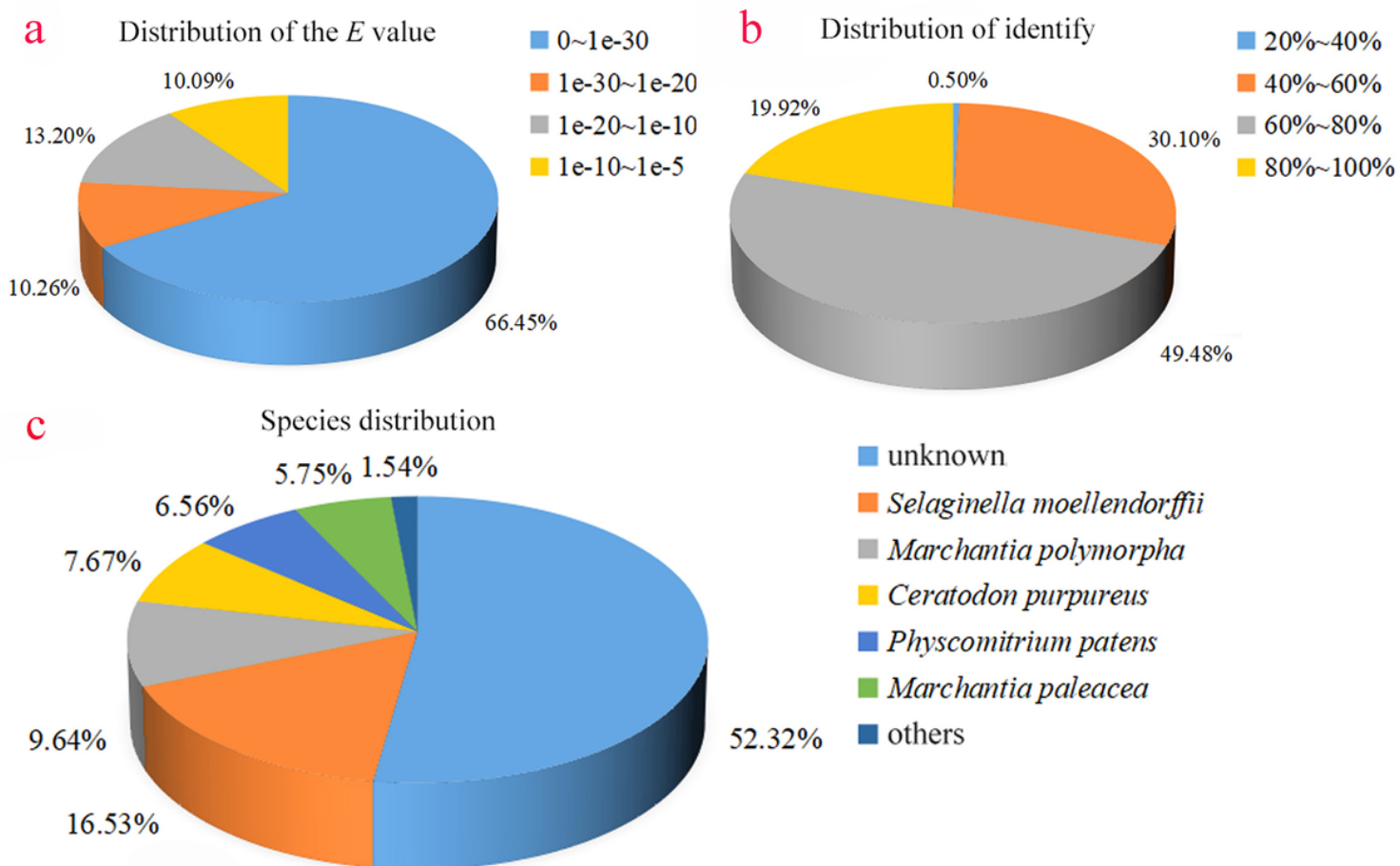
Figure 5

Homologys search of unigenes against NR database of *Gynura divaricata* under NaCl stress.

a, *e*-value distribution of NR annotation; b, distribution of identification; c, distribution of unigenes.
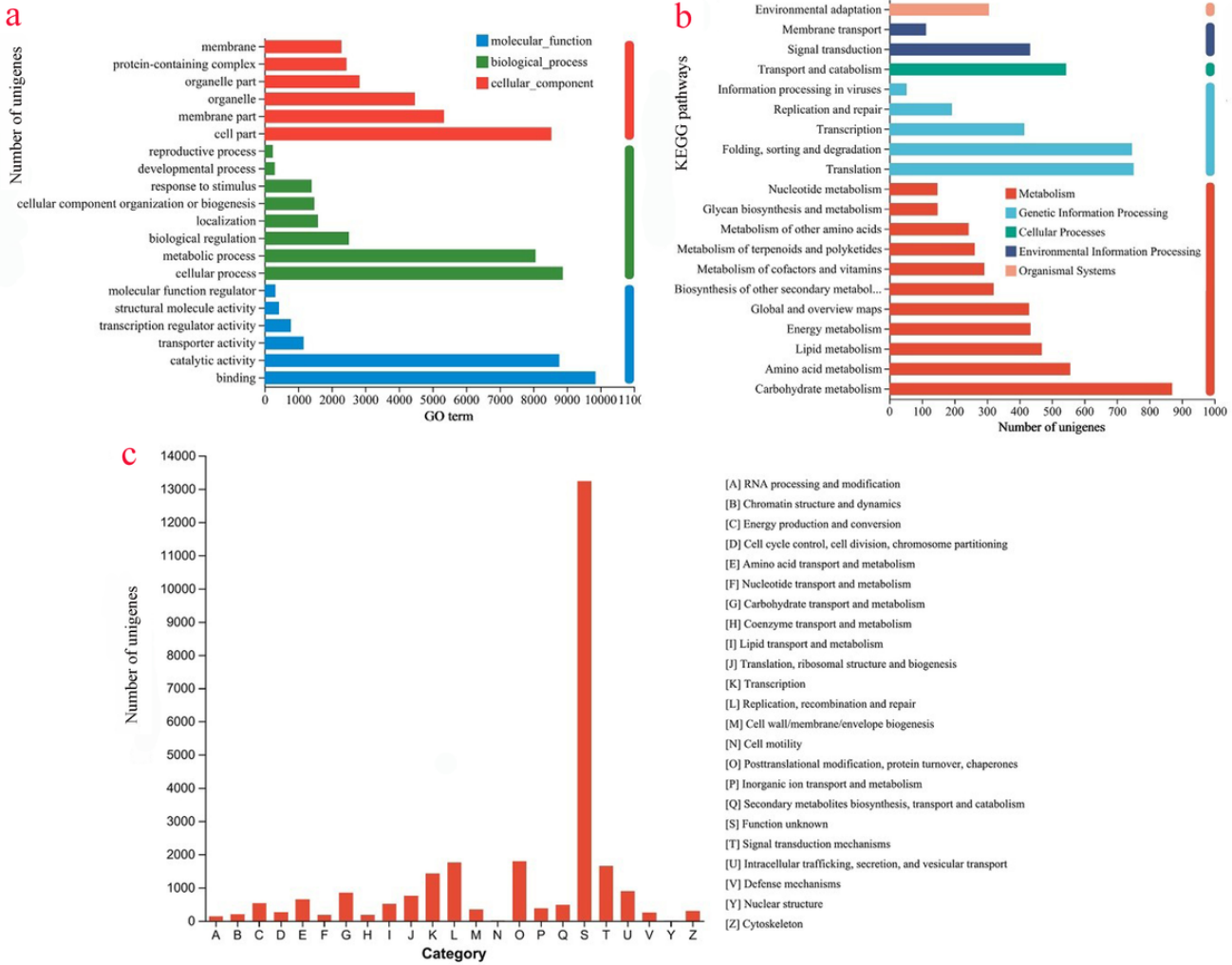
Figure 6

Pathway analysis and functional classification of all unigenes of *Gynura divaricata* under NaCl stress

a, GO classification; b, KEGG pathway; c, COG function classification
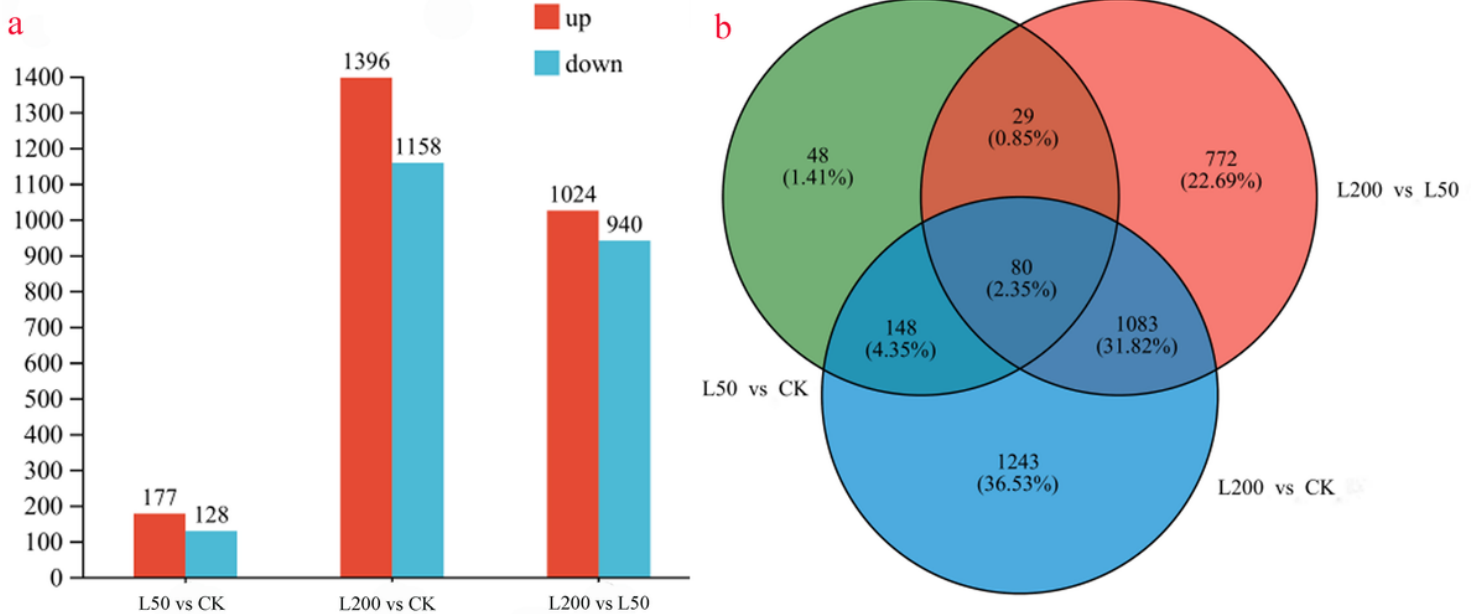
Figure 7

Number of differentially expressed genes (DEGs)(a) in three treatment comparisons and Venn diagram (b) of DEGs of *Gynura divaricata* under NaCl stress.
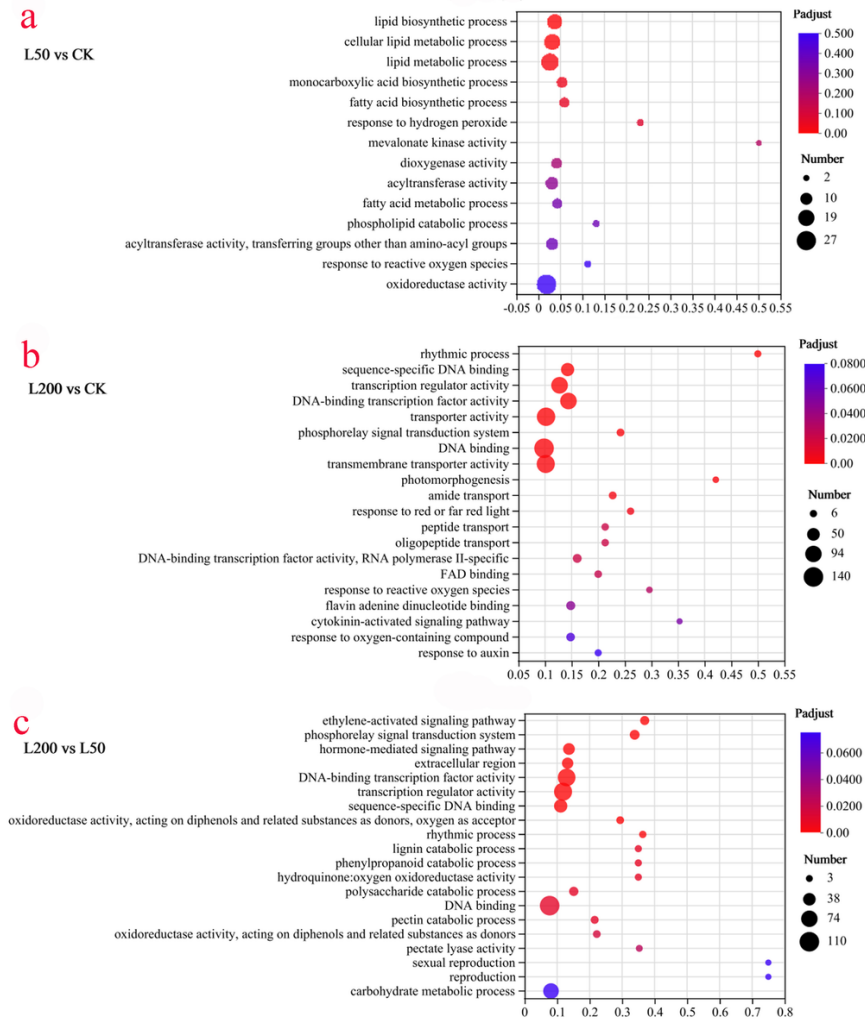
Figure 8

GO enrichment analysis of differentially expressed genes (DEGs) in *Gynura divaricata* leaves under NaCl stress. The size and color of dots indicate the number of DEGs and Padjust, respectively. Padjust < 0.05 indicated asignificantly enriched GO term. a, L50 vs CK; b, L200 vs CK; c, L200 vs L50.
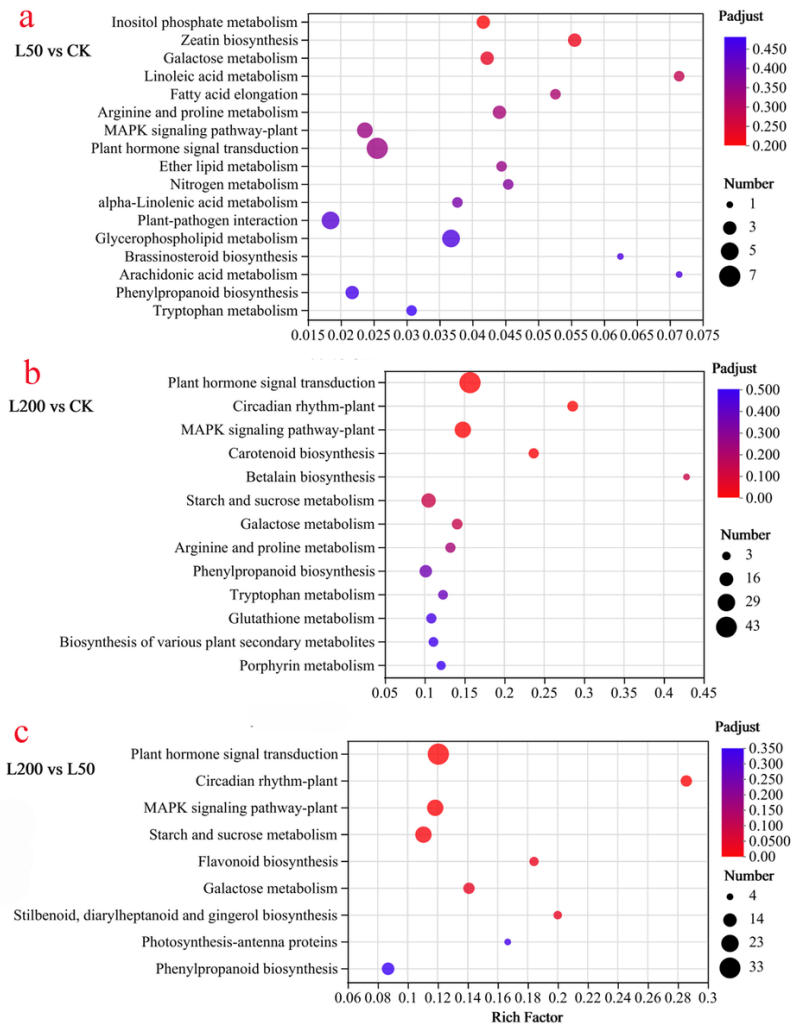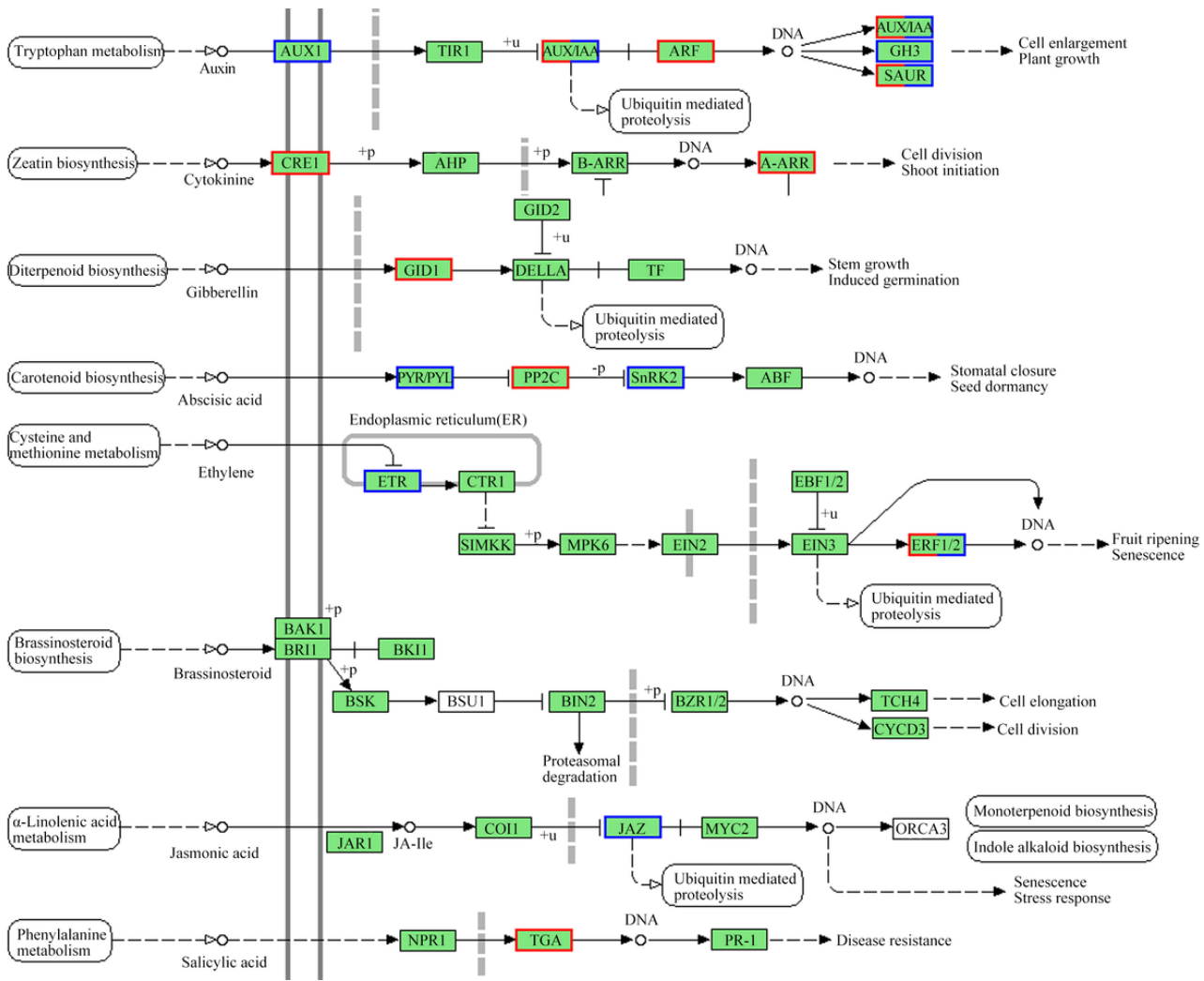
Figure 9

KEGG enrichment analysis of differentially expressed genes (DEGs) in *Gynura divaricata* leaves under NaCl stress. The size and color of dots indicate the number of DEGs and Padjust, respectively. Padjust < 0.05 indicates a significantly enriched GO term. a, L50 vs CK; b, L200 vs CK; c, L200 vs L50.

Figure 10

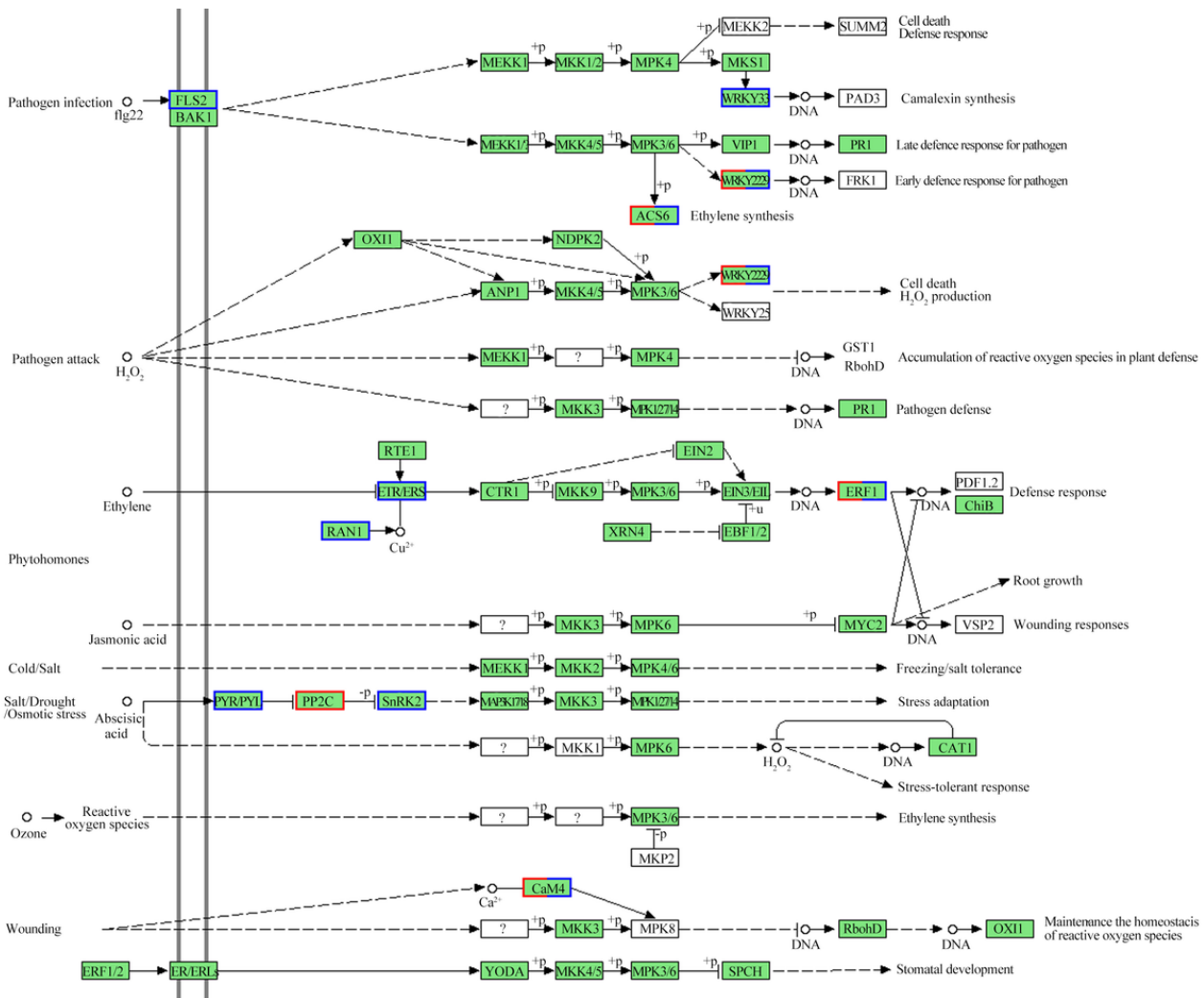DEGs associated with the plant hormone signal transduction pathway (map04075) in *Gynura divaricata* leaves under NaCl stress

Figure 11

DEGs associated with MAPK signaling pathway (map04016) in *Gynura divaricata* leaves under NaCl stress
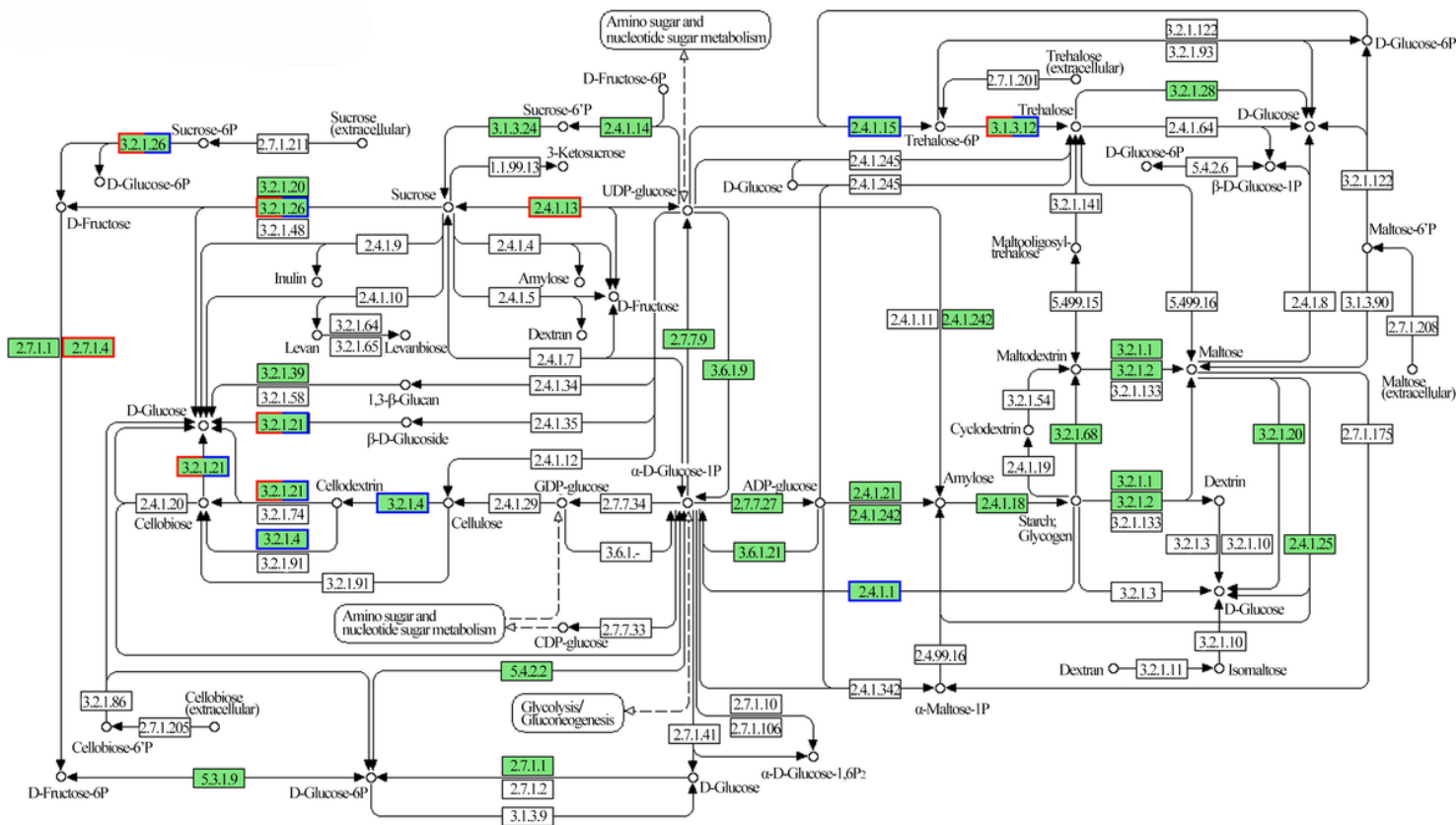
Figure 12

DEGs associated with starch and sucrose metabolism (map00500) in *Gynura divaricata* leaves under NaCl stress.
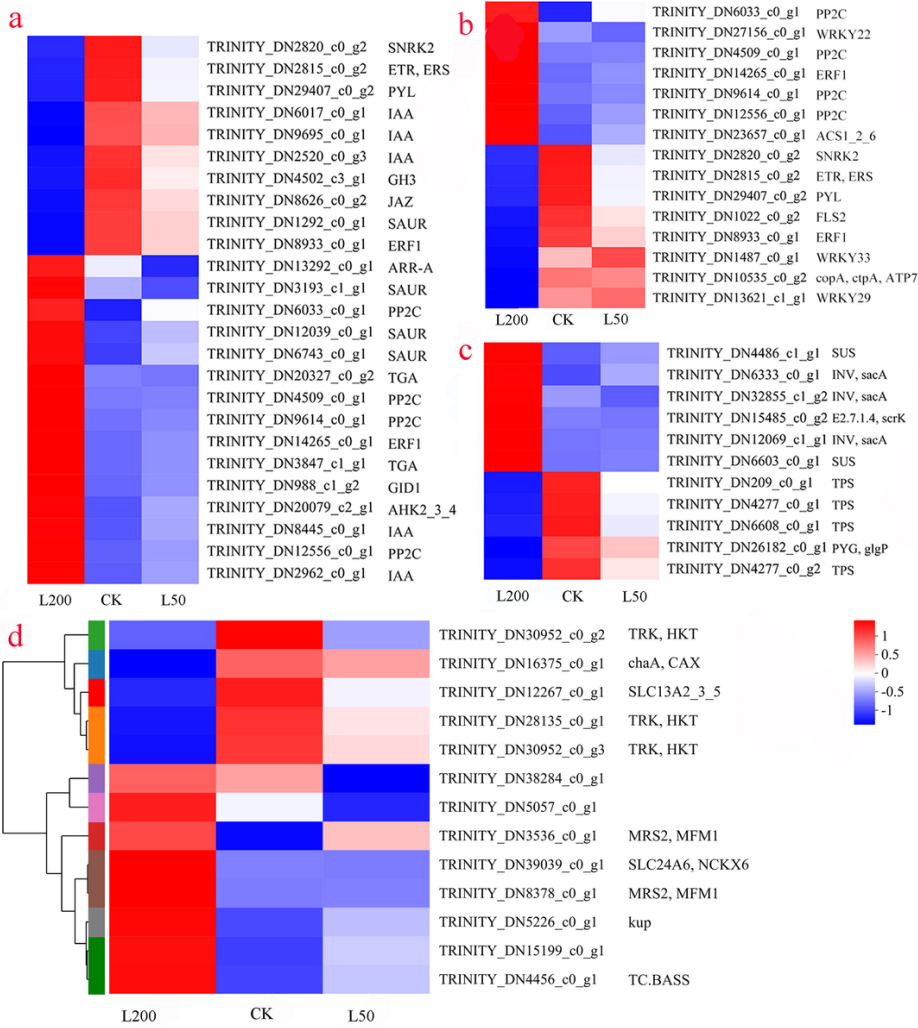
Figure 13

Heatmap of genes related to KEGG processes in *Gynura divaricata* leaves under NaCl stress.

Heatmaps of $\log_2 FC$ of DEGs that were enriched in the MAPK signaling pathway (a), in the plant hormone signal transduction pathway (b), in starch and sucrose metabolism (c), and ion transport (d).
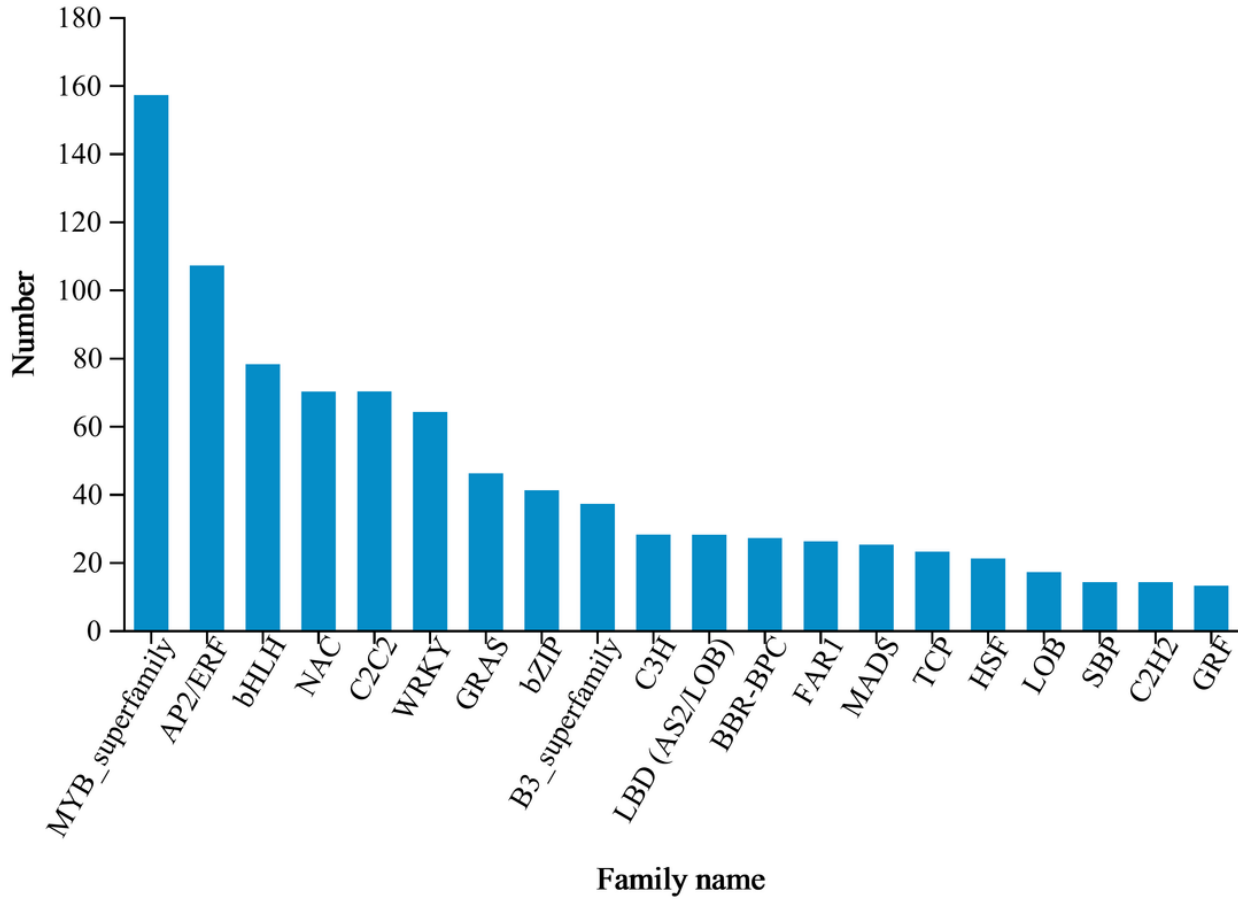
Figure 14

Unigenes coding for transcription factors in *Gynura divaricata* leaves under NaCl stress.
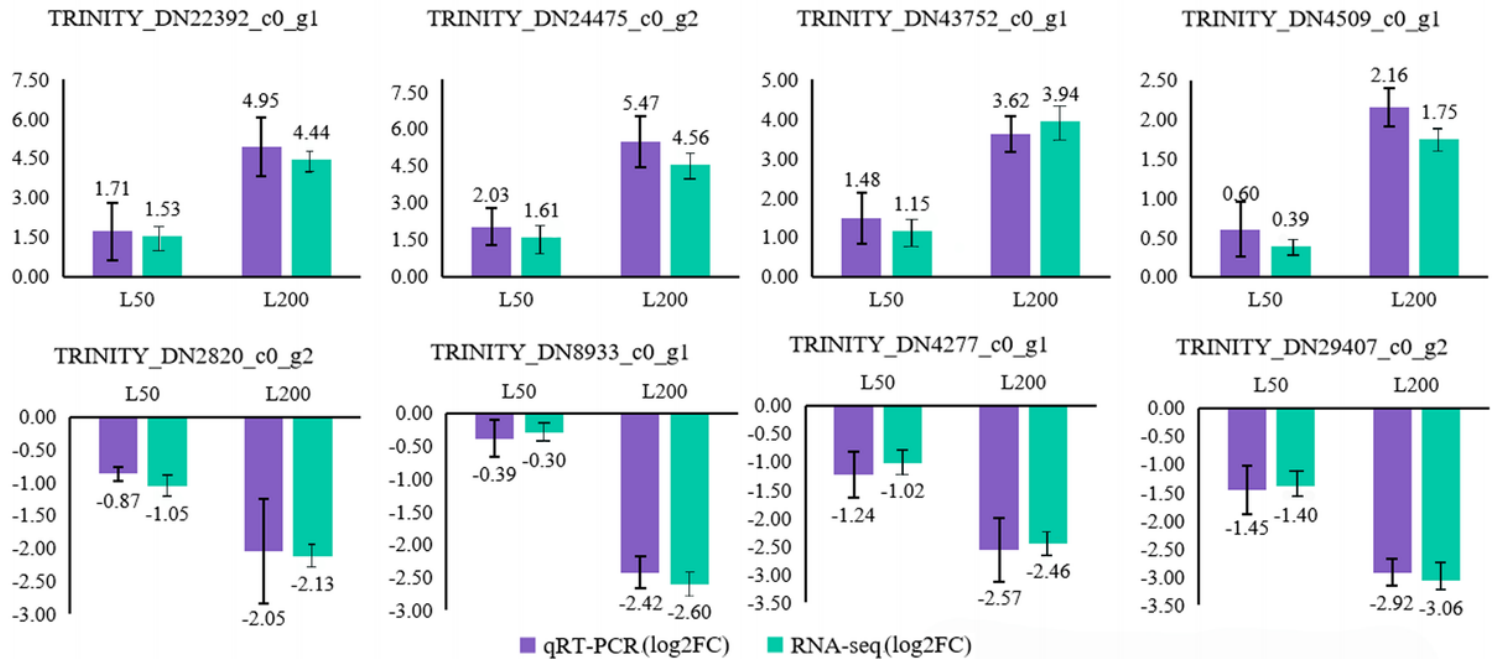

Figure 15

Analysis of the fold changes of eight DEGs assessed by RNA-seq and qRT-PCR. The X-axis represents NaCl concentrations (L50 vs L200) and the Y-axis represents the $\log_2$ fold change. Graphs were generated in Microsoft Excel 2013.

Supplementary Files

This is a list of supplementary files associated with this preprint. Click to download.

- SupplementaryTable1FunctionalannotationofunigeneaccordingtothemajordatabaseofGynuradivaricata.docx